

## Solid-State NMR Investigation of Ligand Mobility and Reactivity in Transition Metal Complexes

Michele R. Chierotti<sup>[a]</sup> and Roberto Gobetto<sup>\*[a]</sup>

**Keywords:** Solid-state NMR / Solid-state mobility / Solid-state reactivity / Transition metal complexes / Ligand fluxionality / Solid-solid reactions / Solid-gas reactions

Solid-state NMR spectroscopy represents a powerful tool to access information on chemical structure, dynamics and reactivity at molecular level on solid compounds and materials. Transition metal complexes represent an unrestricted source of examples for solid-state dynamics and reactivity due to the presence of highly mobile groups, very reactive ligands and the possibility of expanding the coordination sphere. The key question of the influence of the mobility on the reactivity of a system is the occasion for presenting several selected examples of solid-state dynamics and reactivity of transition metal complexes. Although only few unambiguous examples

are reported in which this correlation has been investigated, this review presents the central role of solid-state NMR spectroscopy in the investigation of ligand motion, transformation mechanisms, kinetics and products of solid-state reactions in transition metal complexes. The aim of this microreview is to offer the state-of-the-art on this subject in order to develop new insights and to promote cooperative efforts in this fascinating field.

(© Wiley-VCH Verlag GmbH & Co. KGaA, 69451 Weinheim, Germany, 2009)

### Introduction

The solid state represents a very attractive field of investigation for scientists. The most important feature of a solid is generally considered to be its structure; however, the molecular dynamics and the reactivity in the solid state play

a significant role in determining its chemical properties. As a consequence, besides the innumerable number of papers devoted to the crystalline structure solution or to the physical and spectroscopic property study of the condensed phase, the interest toward motions in closed packed environments and the solid reactivity has received an increasing attention. In transition metal complexes the origin of solid-state dynamics is due to the presence of highly mobile groups, to the electronic structure of the metal center and to synergic effects arising from both ligand and metal. The possibility of expanding the coordination sphere and the

[a] Dipartimento di Chimica I.F.M., Università di Torino, via P. Giuria 7, 10125 Torino, Italy  
Fax: +39-011-6707855  
E-mail: roberto.gobetto@unito.it



*Michele R. Chierotti was born in Torino (Italy) in 1976. He graduated from the University of Torino in 2002 with a thesis researched at the IVIC (Venezuela). In 2006 he received the PhD degrees in Chemical Science working on hydrogen-bonded supramolecular adducts. He spent a period in the Prof. Robin K. Harris's group at the University of Durham (UK). From 2006 he took a postdoctoral position at the University of Torino. His primary research interests are in the areas of organometallic chemistry, polymorphism, hydrogen bond and solid-state NMR spectroscopy.*



*Roberto Gobetto was born near Torino (Italy) in 1956. Graduated in Chemistry, researcher in the Prof. Silvio Aime's group since 1983, he is currently full professor of General Chemistry and Inorganic Chemistry at the University of Torino. He has served as visiting professor at the University of Northridge (California, USA) with Professor Edward Rosenberg and at University of Durham (G.B.) working with Prof. Robin Harris. His main research interests focus on organometallic chemistry, luminescent probes, hyperpolarization and solid-state NMR spectroscopy. He published more than 200 papers on international journals.*

presence of highly reactive ligands allows also a low energy solid-state reactivity. Scientists are trying to manipulate dynamic events at the atomic and molecular scale. The long-standing dream for many researchers is, in effect, the synthesis of compounds whose motions can be triggered and controlled and where molecules behave like “molecular machines” or, at least, like their prototypes.<sup>[1]</sup> This field has experienced a spectacular development in the course of the last decade.<sup>[2]</sup>

Nevertheless, the phenomenon is not at all new for inorganic chemists. Fluxional motions in stereochemically non-rigid transition metal complexes have interested inorganic chemists ever since its discovery in  $[(\eta^1\text{-C}_5\text{H}_5)(\eta^5\text{-C}_5\text{H}_5)\text{-Fe(CO)}_2]$  by Piper and Wilkinson in 1956.<sup>[3]</sup> Transition metal complexes are often dynamic species in solution and even in the solid state. Theoretical studies of molecular conformations and rotational barriers in transition metal complexes have been reviewed by Albright.<sup>[4]</sup> Calculation of the electronic contribution to the internal barrier predict low activation energies for the ring rotation in  $\eta^4$ -cyclobutadienyl-ML<sub>3</sub>,  $\eta^5$ -cyclopentadienyl-ML<sub>4</sub> and  $\eta^7$ -cycloheptatrienyl-ML<sub>3</sub> complexes when dissolved in a solvent. The potential energy for the molecular rotation in the solid state is generally dominated by steric hindrance between nearest-neighbouring molecules. This intermolecular contribution is then strictly related to crystal packing forces. Solid-state dynamics involving ligands bound to transition metals have been extensively reported for:

- a)  $\eta^2$ -olefin,  $\eta^5$ -cyclopentadienyl and  $\eta^6$ -arene,
- b) bent metallocenes and monohapto cyclopentadienyl ligands,
- c) hydride and dihydrogen ligands in mono- and polymetallic systems,
- d) carbonyl and other ligands in mono- and polymetallic systems,
- e) motion of ligands or of the entire molecule when the transition metal complex is located inside a cavity.

Clearly the rotational motion of large rotators is much more affected by the crystalline environment than that of small rotators, such as the methyl group. Braga reviewed in 1992 the dynamic processes in crystalline organometallic complexes affording an overview of the significant papers reported in literature.<sup>[5]</sup> Later the field has been reviewed by K. G. Orrell<sup>[6]</sup> and by B. E. Mann.<sup>[7]</sup>

One may suggest that chemical reactivity in the solid state requires some degree of molecular mobility or the presence of crystal defects. For instance, the mechanism of the solid-gas reaction of the organometallic complex  $[\text{P}(\text{CH}_2\text{CH}_2\text{PPh}_2)_3\text{Co}(\text{N}_2)][\text{BPh}_4]$  with vapour of acetylene, ethylene, formaldehyde, acetaldehyde and carbon monoxide involves and depends on the phosphane ligand motion that allows the N<sub>2</sub> elimination and the organic ligand approach.<sup>[8]</sup> In the field of pharmaceutical compounds, amorphous drugs show significantly higher degradation than analogous crystal forms due to increased mobility.<sup>[9]</sup> Nevertheless in other cases simple correlation between mobility and reactivity cannot be found.<sup>[10]</sup>

The knowledge of molecular structure and solid-state mobility represents an important scientific challenge that can lead to a better design and control of synthetic processes and material performances.

The understanding of the crystal packing of a molecular framework provides information on weak interactions, such as reticular forces and hydrogen bonds (HBs), that govern and drive mobility, transformation and reactivity of this molecule.

For instance, HBs, often, determine the extent of the molecular loosening required for either reorientation processes necessary to undergo the required molecular changes or gas diffusion into reaction sites in solid-gas reactions. On the other hand, a deeper analysis of the mobility and fluxionality involving single groups or entire molecules in a solid can lead to insights into the forces responsible for conformational interconversions and into the factors responsible for solid-state reactions. Furthermore, if it has been evidenced that HBs are the driving forces of many solid-gas reactions<sup>[11]</sup> and solid-state polymorph transformations.<sup>[12]</sup>

Even if many efforts have been done in all these fields, however, there is still the need of increasing the amount of knowledge for a better comprehension of solid phenomena and for a wider technological application on real life problems.

The aim of this microreview is the employment of the potentiality of solid-state NMR techniques to access information at molecular level on dynamics and reactivity of selected organometallic species. In distinct sections, intriguing examples of ligand mobility, solid-gas and solid-solid reactivity and of the influence of the mobility on the reactivity in transition metal complexes will be presented in order to provide a selected overview of the information obtainable from solid-state NMR parameters. Our main goal is to offer the state-of-the-art of these subjects in order to stimulate further future works devoted to answer the key question of whether solid-state mobility is important in determining solid-state reactions involving transition metal complexes.

## NMR Investigation of Mobility and Reactivity in the Solid State

The study of the relationship between molecular mobility and solid-state reactivity usually requires the development of many techniques and new approaches for determining structure features, ligand fluxionalities or overall molecular rotations.

A massive array of experimental methods, based on many different physical phenomena, has been employed on these analyses. Among them, NMR spectroscopy plays a unique role since the availability of several NMR parameters [such as chemical shift, homonuclear and heteronuclear dipolar interaction, chemical shift anisotropy (CSA), relaxation times, lineshape and shielding tensors] allows the investigation of slow and fast dynamic processes, structural environments (HB and nuclear proximities) and solid-state transformations.

Over the last decades new developments in methodology and instrumentation have extended NMR applicability in a large array of solid materials.

### Timescale of Molecular Motions and Solid-State NMR Parameters

Solid-state motions can cover a wide range of correlation times from very fast processes that occur in nanoseconds down to very slow motions of the order of seconds. When monitoring molecular motions, the type and the correlation time of dynamics determine the choice of experiments and techniques. The aim of the dynamic investigation is the quantification of the time scale of the motion and the geometric interpretation of the molecular process. Spectroscopic and diffraction techniques provide information about molecular structure averaged over a particular timescale. For this reason different methods involving elastic and inelastic scattering of particles like electrons, neutrons or photons have been used. In all dynamic processes, parameters such as “contact” time of radiation, excited state lifetime, lifetime of the transient species and data collection time have to be considered.

Local fluctuations in the orientation of various interaction tensors strongly influence relaxation rates, lineshapes and cross-relaxation parameters. The great utility of solid-state NMR lies in its intrinsic sensitivity to cover a wide timescale of a fluxional process ( $10^2$  to  $10^{-10}$  s), see Figure 1.

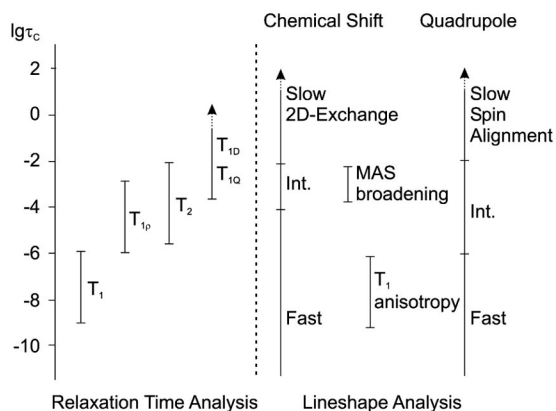


Figure 1. Relationship between the correlation time for a molecular motion and NMR parameters.

No other technique possesses such a wide range of rates over which motions may be examined. Usually, the combined use of XRD and SS NMR methods affords complementary information on both structure and dynamics of solid-state compounds and materials. Indeed the time scale of diffraction techniques is too short ( $10^{-18}$  s) for direct detection of atomic motions, but atomic displacement parameters (ADPs) from XRD contain information about translational, vibrational and rotational oscillations.

We briefly summarize NMR methods for the dynamic process investigation.

Proton resonance lines in solids are mainly broadened by magnetic dipole-dipole interactions with other spins (often protons) in the crystal. Temperature dependence of proton line shapes in wideline experiments and the related measurement of second moment was the simplest way to afford evidence of solid dynamics. Dynamic processes of the order of microseconds can be tackled by spin-lattice relaxation time ( $T_1$ ) measurements, in particular  $^1\text{H}$   $T_1$ , obtained by the well known inversion recovery or saturation recovery.<sup>[13]</sup>

The experimental activation energies obtained from NMR spectroscopic data have been often compared with the values of the potential energy (PE) barriers computed on the basis of the crystallographic data available for the complexes under investigation. These PE barriers related to molecular reorientation are normally computed by using the atom-atom pairwise potential energy method.<sup>[14]</sup>

In principle the spectroscopist can change the Larmor frequency for sampling a wider range of correlation times. Indeed, a field cycling approach has been developed involving fast switches of the polarised signal formed at high magnetic field to the defined lower field in which relaxation is detected.<sup>[15]</sup> This method avoids the low sensitivity limitation at low magnetic fields. However, the requirement of special NMR hardware has strongly limited the number of applications.

Slower motions can be investigated by relaxation time in the rotating frame,  $T_{1\rho}$ .<sup>[16]</sup> The  $T_{1\rho}$  measurement is achieved by inspecting the magnetisation remaining at the end of a spin-lock pulse ( $90^\circ_x$  pulse immediately followed by a pulse of duration  $t_0$  along the axis). Now relaxation measurements are related to the spin-lock field of the order of tens of kilohertz, allowing the extension of dynamic studies to lower frequencies. Alternatively by means of cross polarization pulses, dynamic information can be achieved by heteronuclear  $T_{1\rho}$  measurements, although data interpretation is not straightforward due to the concomitant contribution of both the spin and the molecular relaxation.<sup>[17]</sup>

Other methods are the measurement of heteronuclear  $T_1$ , heteronuclear  $T_{1\rho}$ , X-H cross-relaxation time and proton relaxation time in the dipolar state ( $T_{1D}$ ).<sup>[18]</sup>

The deuterium SS NMR is dominated by the interaction between the nuclear spin and electric quadrupole moment at the nucleus.<sup>[19]</sup>

Motions of X- $^2\text{H}$  bonds and hence, of the quadrupolar tensor, produce variations in the powder pattern of solid samples, i.e. in the distance between the two maxima, with a dynamic range covered by line shape analysis techniques that spans from ca.  $10^4$  to  $10^8$  s $^{-1}$  depending from the QCC (quadrupolar coupling constant) value.

Deuterium  $T_1$  measurements of selectively enriched samples provide an alternative efficient method since they allow the determination of the correlation time and information about the anisotropy associated with the motion in a single set of relaxation data.  $^2\text{H}$  solid echo or quadrupolar echo experiments are usually employed for recording undistorted

spectra in cases in which fast induction decay is present due to strong quadrupolar interaction.<sup>[20]</sup>

Very popular is the investigation of temperature dependence of anisotropic single spin interactions such as chemical shift anisotropy. The interpretation of data involves the use of dynamic models based on ease geometric intuitions. The use of the anisotropic interaction coupled with computing simulations allows the evaluation of the correlation time and of the exchange process topology with the same set of data. In the case of overlapping of anisotropic lines belonging to different chemically inequivalent nuclei, 2D experiments correlating the isotropic peak with the anisotropic chemical shift can be used in order to differentiate in the second dimension the two resonances.<sup>[21]</sup>

The most popular approach for investigating solid-state dynamics is variable temperature high resolution CPMAS experiment. Broadening and interconversion of the static resonances occur when the exchange process rate is of the order of the Larmor frequency difference. Lineshape analysis of high-resolution solid-state NMR recorded at variable temperature affords information on the mechanism and correlation times of molecular motions. Dependence of line widths on the strength of the high-power radiofrequency decoupling field represents an alternative method.<sup>[22]</sup>

Dynamics with correlation times slower than the lifetime of the NMR signals that do not affect the NMR spectrum can be detected by 2D-exchange techniques.<sup>[23]</sup>

A large array of new 2D pulse sequence is now available for spectroscopists, however, a detailed explanation of all these solid-state NMR techniques goes beyond the aim of this review, so, for a complete and rigorous description, the reader should consult authoritative texts.<sup>[24]</sup>

### Analysis of Products Obtained by Solid-State Synthesis

Concerning solid-state reactions, problems arise from the fact that products need to be in crystalline form, possibly single crystals of reasonable size, in order to benefit from the speed and accuracy of single-crystal X-ray diffraction (XRD) experiments. To obtain inter-crystal reactions, the absence of solvent requires, for instance, co-grinding, carried out in a planetary ball mill or with mortar and pestle. On the other hand, the use of finely ground powders favours solid-gas reactions because of the larger surface area. As a consequence, in both cases, crystals tend to shatter into microcrystalline particles as the reaction proceeds, diminishing the usefulness of XRD methods for the characterisation. Thus, the increasing importance of energy-efficient synthesis methods has led to the need for analytical methods not dependent on long-range structural periodicity. Indeed, a severe limitation of XRD stems from the fact that it is not suitable for either amorphous or rather ill-defined solids that lack in crystallinity or for an unambiguous identification of lighter atoms (hydrogen atoms)<sup>[25]</sup> and of their interactions (the HB).<sup>[26]</sup>

As a consequence, one of the drawbacks of these preparations is inherent to the product characterization, which

needs to rely on solid-state spectroscopic techniques such as IR, Raman, DSC, TGA and solid-state NMR spectroscopy.<sup>[27]</sup>

In some cases, the problem can be circumvented by means of seeding, that is, by the use of preformed microcrystals of the desired phase to grow the desired material as crystals of suitable size from solution.<sup>[28]</sup>

When the seeding procedure gives the expected results, traditionally, XRD has been the method of election for studying product structures in the solid state. However, when seeding is not successful, solid-state NMR can often supply the required information, since it does not depend on the presence of long-range translational order, but it is equally applicable to crystalline solids and to poorly crystalline or amorphous materials.<sup>[13,29]</sup>

In the case of solid-state reactions, the analysis is, often, based on the evaluation of differences between reactant and product spectra; this analysis can also reveal molecular species present in the sample such as mixtures, possible side products, intermediate species as well as polymorphs.<sup>[30]</sup>

Several different NMR parameters and experiments provide further information on the product nature and on the reaction mechanism.<sup>[31]</sup> NMR techniques afford:

1. a unique selectivity that allows the differentiation of chemically distinct sites, including protons,<sup>[32]</sup> on the basis of the chemical shift;<sup>[33]</sup>
2. the possibility of investigating the presence (and the strength) of HB from the  $^1\text{H}$  chemical shift of hydrogen bonded signals in  $^1\text{H}$  MAS experiments<sup>[34]</sup> or evaluating the protonation state from chemical shift tensor (CST) values obtained from the analysis of low spinning speed spectra;<sup>[35]</sup>
3. the ability of determining homonuclear ( $^1\text{H}$ - $^1\text{H}$ ,  $^{13}\text{C}$ - $^{13}\text{C}$ , ...) and heteronuclear ( $^1\text{H}$ - $^{13}\text{C}$  and  $^1\text{H}$ - $^{31}\text{P}$ , ...) proximities from 2D spectra;<sup>[36]</sup>
4. the opportunity of obtaining interatomic distances from the analysis of dipolar spinning sideband obtained from recoupling experiments;<sup>[37]</sup>
5. the ability of detecting and characterizing polymorphs and intermediate species from the combined analysis of spectral editing and 2D experiments.

Thus, the combination of solid-state NMR and (single-crystal) XRD analysis in the solid-state transformation study provides in-depth information about the topotactic nature of reactions as well as structural changes that occurred at molecular level.

### Ligand Fluxionality in the Solid State

#### Motion of $\eta^2$ -Olefin, $\eta^5$ -Cyclopentadienyl and $\eta^6$ -Arene

Ethene rotation in solid  $[\text{Rh}(\text{acac})(\text{C}_2\text{H}_4)_2]$  occurs with an activation energy of  $56.5 \text{ kJ mol}^{-1}$  as shown by a combined  $^{13}\text{C}$ ,  $^1\text{H}$ ,  $^2\text{H}$  study of L. G. Butler and co-workers.<sup>[38]</sup>

However, very few examples have been reported in the literature concerning solid-state dynamics of olefin ligands  $\eta^2$ -bonded to a metal. This appears in sharp contrast with the fluxionality of the olefin ligands in the solution state.

Studies on solid-state dynamics involving transition metal complexes were initially focused on Cp and aromatic



rings  $\pi$ -bonded to a metal atom.<sup>[5]</sup> Linewidth, second moment and spin-lattice relaxation times have been extensively used for the evaluation of rotational barriers.<sup>[39–42]</sup>

The greater molecular symmetry involved in Cp and arene systems  $\pi$ -bonded to the metal permits the ring to undergo jumps between equivalent potential energy minima. One may envisage that when the ligand shape is regular and symmetric, smaller barrier between complementary geometries are expected. This idea is quite obvious in solution, but the extent of solid dynamics is determined by quantifying intra- and intermolecular forces present in the crystal.  $2\pi/6$  nearest-neighbor-jumps of benzene moiety have been demonstrated by  $^2\text{H}$  band shape analysis and  $^2\text{H}$   $T_1$  values in  $[\eta^6\text{-C}_6\text{D}_6\text{Cr}(\text{CO})_3]$ .<sup>[43]</sup> Rapid ring rotation was detected also in  $[(\eta^6\text{-C}_6\text{D}_6)_2\text{Mo}]$ , whereas substituted rings such as in the case of  $[\{\eta^6\text{-C}_6\text{D}_3(\text{CD}_3)_3\}_2\text{Mo}]$  are static until 360 K.<sup>[44]</sup>

Solid-state NMR has also been used to detect motion in paramagnetic  $\eta^5$ -cyclopentadienyl and  $\eta^6$ -arene metal systems.<sup>[45]</sup>

The combined use of spectroscopic and crystallographic methods to investigate dynamic processes in crystalline organometallic species has been carefully reviewed by Braga.<sup>[5]</sup> These methods have been jointly applied to the dynamic investigation of pentamethyl cyclopentadienyl complexes of formula  $[(\eta^5\text{-C}_5\text{Me}_5)_2\text{Fe}]$ ,  $[\eta^5\text{-C}_5\text{Me}_5\text{Rh}(\text{CO})_2]$ ,  $[(\eta^5\text{-C}_5\text{Me}_5)_2\text{Cr}_2(\text{CO})_4]$ ,  $[(\eta^5\text{-C}_5\text{Me}_5)_2\text{Fe}_2(\mu_2\text{-CO})(\text{CO})_2]$  and  $[(\eta^5\text{-C}_5\text{Me}_5)_2\text{Rh}_2(\mu\text{-Cl}_2)\text{Cl}_2]$ .<sup>[46]</sup> These ligands display two distinct motions in the solid state: namely the reorientation of the methyl groups around their  $\text{C}_3$  axes and the reorientation of each cyclopentadienyl ligand as a whole around the  $\text{C}_5$  axis. The activation energies for  $\text{CH}_3$  rotation fall in a narrow range (6.5–10.5 kJ/mol) in agreement with limited constraints for the motion. Conversely the activation energies are quite different for the reorientation of permethylated cyclopentadienyl rings due mainly to different intramolecular constraints as demonstrated by atom-atom potential energy barrier calculation. A very interesting case is represented by the low activation value found for the reorientation of the  $\text{C}_5\text{Me}_5$  ligands in  $[(\eta^5\text{-C}_5\text{Me}_5)_2\text{Cr}_2(\text{CO})_4]$  and  $[(\eta^5\text{-C}_5\text{Me}_5)_2\text{Fe}_2(\mu_2\text{-CO})(\text{CO})_2]$  that has been explained by a “synchronous” motion of the methyl group during  $\text{C}_5$  ring motion. In other words PE calculations show that a low energy pathway is available if the motion of the methyl H-atoms “pass over” the CO group of the same molecule during ring reorientation as shown in Figure 2.

A similar correlation of intramolecular motions has been previously suggested for the reorientational motion of  $\text{C}_6\text{H}_6$  and  $\text{C}_2\text{H}_4$  ligands in the cluster complex  $[\text{Os}_3(\text{CO})_9(\mu^2\text{-C}_2\text{H}_2)(\mu_3\text{-}\eta^2\text{-}\eta^2\text{-}\eta^2\text{-C}_6\text{H}_6)]$  in agreement with  $^{13}\text{C}$  CPMAS data.<sup>[47]</sup>

The principal CST values of the ring carbon atoms give further insights into solid-state dynamics of Cp or arene ligands. The principal components of the CST are usually obtained by Herzfeld–Berger analysis of the relative intensity of the spinning sidebands.<sup>[48]</sup>  $\delta_{33}$  is perpendicular to the arene or Cp plane, while  $\delta_{11}$  and  $\delta_{22}$  lie in the plane. Rapid fivefold or sixfold reorientation of the rings results in a

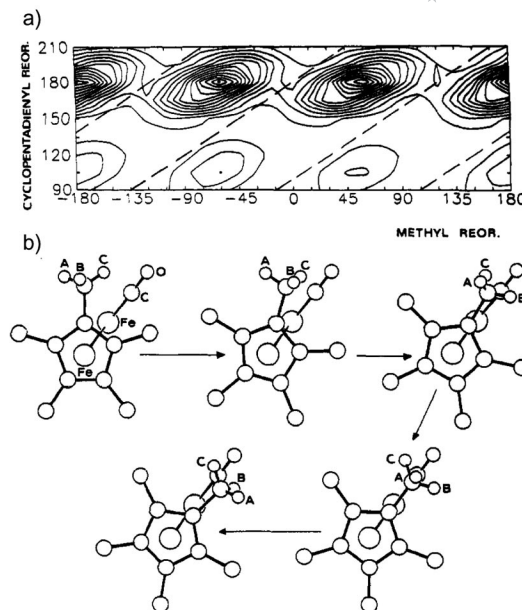


Figure 2. (a) Tridimensional  $\text{PB}_{\text{intra}}$  plot for simultaneous methyl (abscissa) and cyclopentadienyl (ordinate) reorientation in the case of  $[(\eta^5\text{-C}_5\text{Me}_5)_2\text{Fe}_2(\mu\text{-CO})_2(\text{CO})_2]$ . Broken lines represent low-energy paths accessible to the ligand if methyl rotation accompanies cyclopentadienyl reorientation. Contour lines are drawn at  $10\text{ kJ mol}^{-1}$  steps, the minimum being set at  $0\text{ kJ mol}^{-1}$  of the original orientation of the two groups; (b) Schematic representation of the synchronous motion of one cyclopentadienyl ring and of one methyl group in the structure of  $[(\eta^5\text{-C}_5\text{Me}_5)_2\text{Fe}_2(\mu\text{-CO})_2(\text{CO})_2]$ . The methyl “passes over” the terminal group bound to the opposite iron atom.<sup>[46]</sup>

time-averaging of the  $\delta_{11}$  and  $\delta_{22}$  components of the carbon CST.<sup>[49]</sup> Nonaxially symmetric tensors indicates that ring rotation is slow on the timescale of the CST. Then significant difference in the  $\delta_{11}$  and  $\delta_{22}$  values might be a sign of hindered Cp ring rotation, as found for example in the  $[\text{CpNbCl}_4]\cdot\text{THF}$  adduct where intermolecular contacts between the Cl ligands and the nearest H atom on the Cp ring are present.<sup>[50]</sup> The hindered rotation can be intramolecular and/or intermolecular in origin.

A systematic investigation of dynamics in crystalline ansa-metalloocene complexes of formula  $[(\text{C}_5\text{H}_5\text{C}(\text{CH}_3)_2\text{-}(\text{CH}_3)(\text{C}_5\text{H}_4))\text{TiX}_2]$  where  $\text{X} = \text{F}, \text{Cl}, \text{Br}, \text{or I}$  has been reported by K. Prout et al.<sup>[51]</sup> Only a combination of VT 1D and 2D magnetisation transfer experiments, line shape simulations of exchange broadening phenomena,  $^2\text{H}$  NMR wideline studies allowed the complete interpretation of molecular dynamics of these systems. Interestingly, the exchange mechanism in the solid state is rather different from the enantiomeric exchange process observed in solution. In the crystalline state at  $180^\circ$  reorientation about the pseudo- $\text{C}_2$  axis bisecting the  $\text{X-Ti-X}$  interbond angle occurs with a concomitant polytopal relaxation about the metal centre. This motional event of large angular extent is quite rare if compared with most of the motions in molecular crystals where only individual segments of molecules are engaged in dynamic processes. It is also worth noting that the reported motion for ansa-titanocenes appears to be intermediate be-

tween the isotropic overall molecular reorientational disorder characteristic of a crystalline phase and the fluxionality of specific groups within the molecule.

Rotation of  $\eta^5$ -C<sub>6</sub>H<sub>7</sub> and  $\eta^5$ -C<sub>7</sub>H<sub>9</sub> rings have been reported for  $[\eta^5\text{-C}_6\text{H}_7\text{Fe}(\text{CO})_3]\text{BF}_4$  and  $[\eta^5\text{-C}_7\text{H}_9\text{Fe}(\text{CO})_3]\text{BF}_4$ .<sup>[52]</sup> In both cases rapid reorientation of the rings and fast exchange of the carbonyl ligands have been demonstrated by a <sup>1</sup>H/<sup>13</sup>C variable temperature study.

### Motion of Monohaptocyclo-Pentadienyl Ligands

2D exchange experiments can afford insights about the mechanism of orientation since they provide information simultaneously about all exchanging sites. This is the case for intramolecular rearrangement of monohaptocyclopentadienyl rings in  $[\text{M}(\eta^5\text{-C}_5\text{H}_5)_2(\eta^1\text{-C}_5\text{H}_5)_2]$  (M = Ti and Hf) that proceeds via a sigmatropic shift.<sup>[53]</sup>

More interesting fluxional motions in the slip-sandwich structure of solid decamethylzincocene  $[(\eta^5\text{-C}_5\text{Me}_5)\text{Zn}(\eta^1\text{-C}_5\text{Me}_5)]$  have been investigated by a combination of NMR methods.<sup>[54]</sup> Variable temperature <sup>13</sup>C CPMAS and static powdered <sup>2</sup>H NMR spectra of  $[(\eta^5\text{-C}_5\text{Me}_5)\text{Zn}(\eta^1\text{-C}_5\text{Me}_5)]$  allow the detection of the different processes reported in Figure 3.

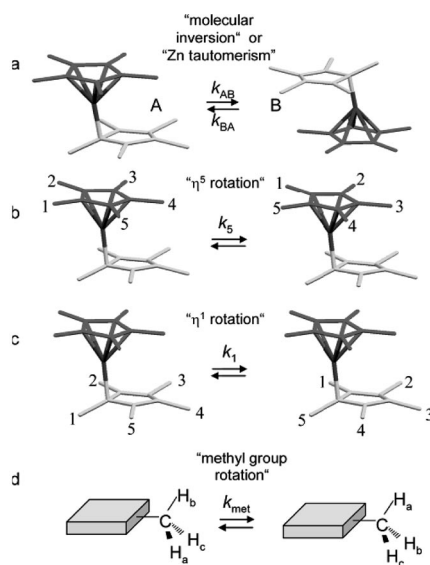


Figure 3. Fluxional motions observed in  $[(\eta^5\text{-C}_5\text{Me}_5)\text{Zn}(\eta^1\text{-C}_5\text{Me}_5)]$ . (a) The molecular inversion process or Zn tautomerism: interchange the role of both ring  $\eta^5$  and ring  $\eta^1$  by the Zn tautomerism between the two equivalent positions. The overall result is equivalent to an inversion of the molecule. In (b) and (c), the  $\eta^5$  and  $\eta^1$  rotation processes are shown. (d) Methyl group rotation corresponding to 120° jumps.<sup>[54]</sup>

Fast rotations of both permethylated cyclopentadienyl rings have been detected down to 156 K. There is also an order-disorder phase transition around 210 K. The disorder is shown to be dynamic arising from a fast combined Zn tautomerism and  $\eta^1/\eta^5$  reorganization of the Cp\* rings between two degenerate states A and B related by a molecular inversion.

### Motion of Hydrides and Dihydrides

Nuclear magnetic resonance spectroscopy has had extensive applications for the characterization of numerous metal-hydrogen systems. Molecular motion of interstitial hydrides in transition metal systems has received increasing attention in recent years, mainly for the key role of hydrogen mobility and hydrogen-storage in the development of possible application in energy industry (i.e. light-weight battery material in cars, portable devices, etc.). Although the greatest emphasis of proton NMR has been to evaluate diffusion behavior of hydrogen nuclei on alloys,<sup>[55]</sup> also hydrides in transition metal clusters have been investigated. For example spectral behaviours of VT <sup>1</sup>H NMR wide-line spectra of powdered  $\text{HRu}_{10}\text{C}(\text{CO})_{24}^-$  may be explained by hopping of the hydride between the interstitial "cap" sites in the ruthenium compound when the temperature is above 250 K. Solid-state NMR measurements coupled with relaxation time data were fundamental in demonstrating motional process involving hydrides in solid  $[\text{H}_4\text{Ru}_4(\text{CO})_{12}]$ <sup>[56,57]</sup> and  $[\text{H}_4\text{Ru}_4(\text{CO})_{11}\text{P}(\text{OMe})_3]$ .<sup>[57]</sup>

Even more interesting are the motion of  $\eta^2$ -dihydrogen complexes. <sup>2</sup>D solid-state NMR spectroscopy represents the investigation technique of choice in the intermediate regime of motion, typical for  $\eta^2$ -systems in which the interproton distance is in the range 0.90–1.6 Å. Changes in the orientation of the quadrupolar tensor with respect to the external magnetic field represent a very sensitive probe for the investigation of nuclear motions. For a comprehensive overview of the field, the reader is referred to the recent review of Buntowsky and Limbach.<sup>[58]</sup>

### Motion of Carbonyl and Other Ligands

In solution state carbonyl ligands are often very fluxional in polymetallic systems due to the presence of low energy processes involving coordination change of CO from terminal to  $\mu_2$ - or  $\mu_3$ -bridging. Fluxional motions of carbonyls in the solid state are quite rare: for  $\text{Fe}_3(\text{CO})_{12}$  the presence at room temperature of only six resonances in the <sup>13</sup>C MAS spectrum is not consistent with the presence of ten terminal and two bridging carbonyls.<sup>[59]</sup> Only at low temperature the <sup>13</sup>C spectrum agrees with the X-ray structure. The comparison of the experimental values of exchange-averaged shielding tensors from the slow-spinning MAS experiment with the values calculated for a two-site exchange model provides evidence for the interpretation of the exchange mechanism occurring in the solid  $\text{Fe}_3(\text{CO})_{12}$  cluster. The X-Ray structure exhibits an inversion disorder with two enantiomers occurring with equal probability. These two orientations can be interconverted by a 60° rotation of the iron triangle within the distorted icosahedron defined by the carbonyl ligands. Johnson, Braga and co-workers<sup>[60]</sup> suggested that fluxional behaviour can also be explained as small librations involving the metal polyhedron and the carbonyl framework.

<sup>13</sup>C and <sup>31</sup>P NMR spectroscopic data obtained over a range of temperature for  $[\text{W}(\text{PMe}_3)_3\text{H}_6]$  show chemical ex-

change between the phosphane ligands. Line shape analysis and magnetization transfer experiments afford Arrhenius activation parameters for the ligand fluxionality interchange ( $E_a = 148.8 \pm 15 \text{ kJ mol}^{-1}$  and  $A = 6.6 \times 10^{23} \text{ s}^{-1}$ ).<sup>[61]</sup>

Any kind of mechanism involving spatial permutation of the phosphane ligand should have a higher activation barrier in the solid state. However, the relatively low energy pathway founded can be explained by a “double rearrangement mechanism” of the tricapped-trigonal-prismatic geometry with an interconversion that involves a mono-capped-square-antiprismatic geometry and a tricapped-trigonal-prismatic intermediate in which all phosphane ligands occupy capping positions as depicted in Figure 4.

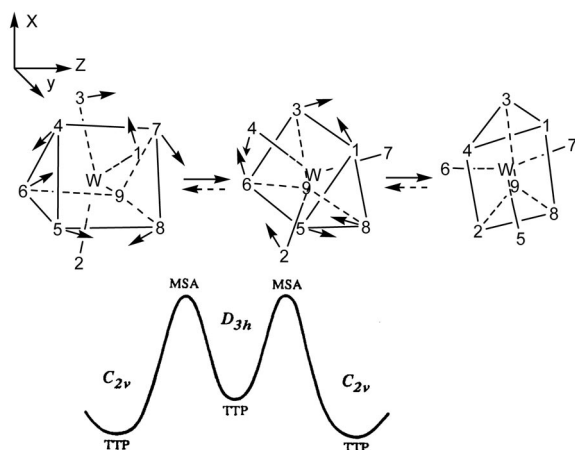


Figure 4. Energy profile for the rearrangement and proposed “double stretch” mechanism that affects ligand functionality interchange. The numbers 1, 3, 5, 6, 8, and 9 represent hydrogen atoms while the numbers 2, 4, and 7 represent phosphorus atoms.<sup>[61]</sup>

In such mechanism a complete scrambling of the ligand functionality is obtained with a relatively small movement of phosphane ligands within the crystalline frame.

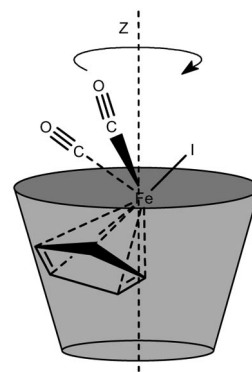
Other examples have been recently reviewed by Bernard and Wasylishen.<sup>[62]</sup>

### Motion Inside a Cavity

Lower activation energy barriers are expected for the motion of transition metal complexes when included into cavities created by host molecules such as cyclodextrin (CD), zeolites, alluminosilicates, etc. Indeed, many authors have reported on rotation of molecules, or of part of them, included either in CD and zeolites. Their motion depends on the symmetry, size and orientation of the guest molecule within the host cavity. Furthermore the possibility of formation of host-guest weak interactions plays a fundamental role in determining the motion kind and regime and reactivity.<sup>[63]</sup>

One dimensional switching-angle sample spinning NMR measurements demonstrated that the ferrocene molecule precess with a precession angle of  $69^\circ$  in  $\gamma$ -CD cavity.<sup>[64]</sup> In  $\beta$ -CD, three kinds of ferrocene molecules were enclathrated, in different motional states, with populations of 0.42, 0.32 and 0.26, respectively; ferrocene I is tightly enclathrated and

rotates around its fivefold axis, whereas ferrocenes II and III precess with precession angles of  $30^\circ$  and  $42^\circ$ , respectively.  $\text{Cr}(\text{CO})_6$  in  $\gamma$ -CD shows isotropic reorientation as demonstrated by the single carbonyl resonance without spinning sidebands at low spinning rate compared to the rigidity of crystalline  $\text{Cr}(\text{CO})_6$ , testified by the presence of four isotropic resonances with a large spinning sideband manifold.<sup>[65]</sup> Transition metal carbonyl complexes containing  $\pi$ -bonded ligands show a more complicate dynamics when included in CD cavities.  $[(\eta^6\text{-C}_6\text{H}_6)\text{Cr}(\text{CO})_3]$  does not rotate isotropically inside the cavity, but a  $\text{C}_6$  rotation around the main molecular axis of symmetry has been suggested on the basis of  $^{13}\text{C}$  carbonyl and deuterium data of samples selectively enriched in  $^{13}\text{C}$  (carbonyl ligand) and  $^2\text{D}$  (arene ligand) respectively.<sup>[66]</sup> In several cases the shape of the guest, the size of the host and the strength of the intermolecular forces allow the rotation of the entire molecule only along certain axis. Then the analysis of the spinning sideband manifold of the carbonyl resonances that affords the CST components provides a clear insight on the specific motion involving the ligand (i.e. carbonyl) or the entire molecule into the cavity. The comparison between spinning sideband manifolds of crystalline  $[(\eta^5\text{-C}_5\text{H}_5)\text{Fe}(\text{CO})_2\text{I}]$  and  $[(\eta^5\text{-C}_5\text{H}_5)\text{Fe}(\text{CO})_2\text{I}]$  included in  $\beta$ -CD demonstrates the presence of a precessional motion of the organometallic complex in the host-guest adduct in the solid state with a  $\beta$ -angle of a  $49^\circ$  with respect to the main symmetry  $Z$  axis of the CD cavity as shown in Scheme 1.<sup>[67]</sup>



Scheme 1.

An unusual dynamic behavior has been reported for an other half sandwich iron complex, namely  $[(\eta^5\text{-C}_5\text{H}_5)\text{Fe}(\text{CO})_2\text{CH}_3]$ . In this case the situation is reversed, since the pure compound is much more mobile due to the plastic crystal-like behavior, whereas when included in the CD cavity of the  $\beta$ -CD, the shape of the guest and the size of the host do not allow an isotropic motion, but only rotation of the entire molecule along a  $\beta$ -angle of  $51^\circ$  (Figure 5).

An intriguing case is represented by  $[(\eta^5\text{-C}_5\text{H}_5)_2\text{Mo}_2(\text{CO})_6]$  included in  $\gamma$ -CD where the  $^{13}\text{C}$  CPMAS NMR VT spectra show subtle yet important differences compared to the analogous spectrum recorded for the pure crystalline  $[(\eta^5\text{-C}_5\text{H}_5)_2\text{Mo}_2(\text{CO})_6]$ .<sup>[67]</sup> Fast motion of one  $(\eta^5\text{-C}_5\text{H}_5)\text{Mo}(\text{CO})_3$  part inside the CD cavity has been suggested,



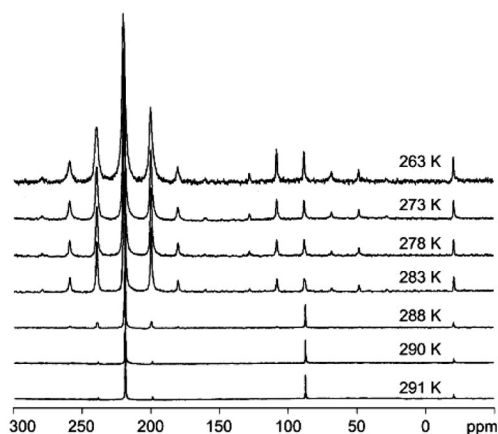


Figure 5. VT (263–291 K)  $^{13}\text{C}$ -CPMAS NMR spectra of crystalline  $[(\eta^5\text{-C}_5\text{H}_5)\text{Fe}(\text{CO})_2\text{CH}_3]$  recorded at 100.64 MHz with a spinning speed of 10 kHz.<sup>[67]</sup>

whereas the other half part of the dimer non-included in the CD cavity appears rigid due to the presence of strong interatomic interaction with neighbouring molecules.

## Reactivity in the Solid State

Reactions occurring in the solid state, such as that among solid reactants or between a solid and a vapour, often provide fast and quantitative routes to the preparation of novel organic, inorganic and organometallic compounds.<sup>[68]</sup>

In recent years, under the impetus of crystal engineering,<sup>[69]</sup> solvent-free processes have begun to be investigated for the preparation of crystalline materials,<sup>[70]</sup> molecular co-crystals,<sup>[71]</sup> coordination networks<sup>[72]</sup> and salts.<sup>[73]</sup>

The interest toward this type of reactions is three fold: a) in the field of the Green Chemistry from an environmental point of view, b) because they provide new synthetic opportunities and c) because they represent a scientific challenge. Indeed, they do not need the use of solvents, avoiding problems concerning their storage and disposal, and furthermore, they frequently give products that differ from those obtained by conventional methods, with high yields (often 100%) and without any requirement of purifying workup.

Recent reviews collect many waste-free reactions from virtually all fields of organic,<sup>[68h]</sup> organometallic<sup>[74]</sup> and inorganic<sup>[29,75]</sup> synthesis with about 100% yield in stoichiometric runs.

Solid-state reactions differ from reactions in solution essentially in the fact that they occur within the constraining environment of the reactant crystal lattice. This, together with the interplay of weak interactions and dynamics, affects the molecular loosening and molecular change steps, controlling both kinetics and the nature of the products.<sup>[76]</sup> The final result, therefore, may not necessarily be the thermodynamically most stable product available, but rather the product of reaction pathways accessible in the environment

of the solid. Thus, one of the best examples of these effects is the enhanced chemical reactivity of amorphous materials. These amorphous substances will then easily react due to their increased mobility and ability to interact with vapours or solids. Although amorphous materials can be intrinsically interesting, information is often required about the structure of phases or compounds and about formation or decomposition mechanisms.

For this reason there was much effort to look for “topochemical reactions”, i.e. single-crystal-to-single-crystal reactions without crystal disintegration.<sup>[77]</sup> However, they appear to be only possible if the shape of the product molecules do not significantly deviate from the starting molecules in the crystal.<sup>[78]</sup> Since these conditions are almost never met, only few examples could be found, while the majority of solid-state reactions proceed with crystal disintegration at low to medium conversion.<sup>[79]</sup>

In the following, we will focus on the role and the ability of solid-state NMR in characterizing solvent-free processes of transition metal complexes: those involving gas uptake by a molecular crystal to form a new crystalline solid and those involving reactions between molecular crystals or between a molecular and an ionic crystal to yield new crystalline materials.<sup>[28,80]</sup>

## Gas-Solid Reactions

How can a reaction between a solid substrate and a gaseous reactant proceed? As stated above, the crystal packing determines the extent of molecular loosening required for gases to diffuse to the reaction site in solid-gas reactions. In principle, one may envisage two possible pathways. (a) The crystalline solid is loosely packed allowing small gaseous molecules to diffuse and flood the whole solid through its channels. (b) The gaseous molecules react at the surface of the solid disrupting the crystalline order and allowing more gaseous reactant to penetrate interlayer spaces and to interact with further substrate molecules. To get bulk reactivity, such a process may require the sliding of the product species over the solid surface. Thus, this reaction can only proceed if two requirements are met: (i) the surface reaction is spontaneous, and (ii) the reaction product separates from the solid substrate. Alternatively, the transformation of the uppermost layer can cause an “expansion” of the lattice, thus allowing the gaseous reactant to disperse into it.

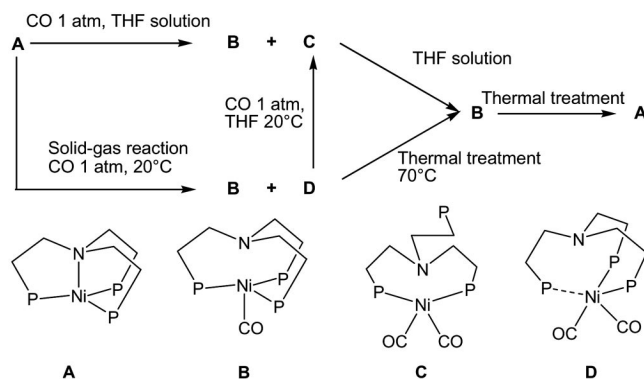
In the last 20 years systematic studies have been undertaken to design organometallic complexes capable of reacting in the solid state at molecular level, with both inorganic and organic gaseous molecules.<sup>[81]</sup>

As far as possible applications are concerned, a better knowledge of solid-gas reactions may provide useful insights into the design of novel sensor devices for gases. Furthermore, the investigation of stoichiometric transformations of organometallic solids may lead to the development of catalytic reactions in the solid state; this would be a viable alternative to heterogeneous catalysis using organometallic compounds supported on inorganic surfaces.<sup>[82]</sup>



A series of papers in which solid-state NMR has been used for clarifying the mechanism of solid-state reactions and structural features of the products have been published.

Solution and solid-gas reactions of the trigonal pyramidal  $\text{Ni}^0$  complex  $[\text{Ni}(\text{NP}_3)]$  (**A**) with CO [ $\text{NP}_3 = \text{N}(\text{CH}_2\text{CH}_2\text{PPh}_2)_3$ ] (Scheme 2, a) have been investigated.<sup>[83]</sup> Depending on the reaction environment, i.e. in solution or solid-gas, the product can be the monocarbonyl **B**, the dicarbonyl **C** or **D** species, where **D** has the same stoichiometry as **C**, but exhibits a different  $^{31}\text{P}$  CPMAS spectrum (Scheme 2, b). As the reaction proceeds it has been observed a progressive decrease of  $^{31}\text{P}$  CPMAS signals related to the parent compound **A** with concomitant formation of **B** and the upsurge of the **D** resonances centred at about 12, 0 and  $-23$  ppm.



Scheme 2.

The significant differences in  $^{31}\text{P}$  NMR patterns, the minor stability of **D** with respect to **C** as well as the similarity of their IR and DRIFT spectra, strongly suggest that **D** represents a metastable or activated species (not observable in solution) in which a phosphane arm from  $\text{NP}_3$ , although unfastened, is located close to the metal centre as a consequence of the constraining environment of the crystal lattice. The proximity of the free phosphane arm to nickel makes solid **D** capable of losing one CO ligand, thus converting to **B**. Unlike in solution, the latter compound undergoes thermal dissociation of CO in the solid state to generate the starting complex **A**.

In light of the experimental evidence, it has been concluded that the addition of one CO to **A** to form **B** can occur in the solid state with small rearrangements around the metal centre, i.e. without an extensive alteration of the overall crystal lattice. In contrast, the further transformation of **B** to **C**, in which the free phosphane arm is expected to lie far away from the metal,<sup>[84]</sup> would produce changes not tolerable in the solid. Indeed, the formation of the thermodynamically more stable **C** form in the solid state would cause an increase in the crystal volume, which in fact is not expected for a solid-gas reaction, as elegantly shown by Siedle through BET nitrogen physisorption experiments.<sup>[81d]</sup>

In principle, for organometallic compounds one would expect solid-gas reactions to take place readily and easily if the solid substrate is coordinatively unsaturated or if “lightly stabilized” ligands are present.<sup>[85]</sup> This behaviour

has been shown in solid-state reactions of the coordinatively unsaturated  $[\text{H}_2\text{Os}_3(\text{CO})_{10}]$  ( $46 e^-$ ) with gaseous Lewis bases **L** ( $\text{L} = \text{CO}, \text{NH}_3, \text{H}_2\text{S}$ ).<sup>[86]</sup>

The complex  $[\text{H}_2\text{Os}_3(\text{CO})_{10}]$  ( $46 e^-$ ) reacts with gaseous Lewis bases **L** affording the electron saturated adducts  $[\text{H}_2\text{Os}_3(\text{CO})_{10}\text{L}]$  ( $48 e^-$ ). This paper represents a rare case in which  $^1\text{H}$  MAS NMR has been used for characterizing hydride species: their chemical shift, far from those of aliphatic and aromatic protons, opens unexpected opportunities, for proton investigation in organometallic compounds, as for the well known HB characterization (see below).

For the reaction of  $[\text{H}_2\text{Os}_3(\text{CO})_{10}]$  with CO, the solid product  $[\text{H}_2\text{Os}_3(\text{CO})_{11}]$  was unambiguously characterized by means of high-resolution  $^1\text{H}$  MAS and  $^{13}\text{C}$  (solution) NMR spectra. Two relatively sharp signals at  $-20.1$  and  $-10.5$  ppm (Figure 6) for bridging and terminal hydride, respectively, confirmed the proposed structure in agreement with solution data. Upon longer reaction times  $[\text{H}_2\text{Os}_3(\text{CO})_{11}]$  releases  $\text{H}_2$  and transforms mainly into  $[\text{Os}_3(\text{CO})_{12}]$ .

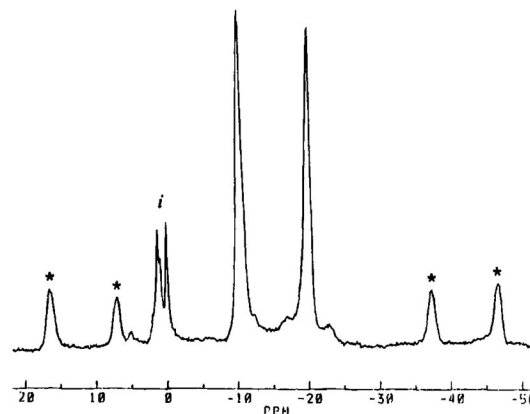


Figure 6.  $^1\text{H}$  MAS NMR spectrum at 300 MHz of  $[\text{H}_2\text{Os}_3(\text{CO})_{11}]$  with a spinning speed of 8 kHz. The asterisks denote the spinning sidebands flanking the isotropic peaks; *i* indicates residual solvent impurities.<sup>[86]</sup>

Solid-state NMR in the last years has found many applications also in the field of Surface Organometallic Chemistry (SOMC), the branch of the chemistry devoted to design and prepare single-site heterogeneous catalysts.<sup>[87]</sup> Indeed, one of the critical aspects of this field is to define the structure of the surface complex at molecular level and to investigate the reaction pathway leading to grafted species. This allows structure-activity correlations, and thereby a rational improvement of targeted catalysts. However, this challenging task still remains rather difficult, but recent development of advanced spectroscopic techniques has greatly helped to characterize the exact nature of active sites of the systems, their formation mechanism and also their solid-gas reactivity.<sup>[88]</sup>

For instance, it has been reported the reaction of  $[\text{Ru}_3(\text{CO})_6(\mu\text{-CO})(\mu_3\text{-}\eta^2\text{-}\eta^3\text{-}\eta^5\text{-C}_{12}\text{H}_8)]$  physisorbed on  $\text{SiO}_2$  with CO in the solid state.<sup>[89]</sup>  $[\text{Ru}_3(\text{CO})_6(\mu\text{-CO})(\mu_3\text{-}\eta^2\text{-}\eta^3\text{-}\eta^5\text{-C}_{12}\text{H}_8)]$  reacts readily in solution with CO quantitatively affording  $[\text{Ru}_3(\text{CO})_{12}]$  and free acenaphthylene. However,

this reaction is considerably inhibited in the solid state at room temperature. Contrastingly, by physisorbing  $[\text{Ru}_3(\text{CO})_6(\mu\text{-CO})(\mu_3\eta^2:\eta^3:\eta^3\text{-C}_{12}\text{H}_8)]$  on a surface of  $\text{SiO}_2$  ( $450\text{--}550\text{ m}^2\text{ g}^{-1}$  surface area, 10% coverage of the silica surface) the same reaction occurs readily. The  $^{13}\text{C}$  CPMAS spectrum of  $[\text{Ru}_3(\text{CO})_6(\mu\text{-CO})(\mu_3\eta^2:\eta^3:\eta^3\text{-C}_{12}\text{H}_8)]$  physisorbed on  $\text{SiO}_2$  shows the bridging carbonyl at  $\delta = 270$  ppm, while the six terminal CO resonances overlap in three broad signals at 205, 190 and 185 ppm respectively. On following the reaction with CO by high proton power decoupling (HPPD)  $^{13}\text{C}$  MAS there is a progressive decrease in the intensity of the resonances of the starting material, which are in turn replaced by an intense peak at  $\delta = 199.8$  ppm unambiguously assigned to  $[\text{Ru}_3(\text{CO})_{12}]$ . The reduction in the chemical shift anisotropy of this signal compared to that of crystalline compound gave information on the fluxionality of the CO (see above).

Rataboul et al. have shown how 1D and 2D multinuclear solid-state NMR techniques can be fundamental in probing at molecular level surface structures of complexes grafted on the silica surface.<sup>[90]</sup> They have reported the characterization by 1D and 2D multinuclear techniques of the grafted complex  $[(\equiv\text{SiO})\text{Zr}(\text{CH}_2\text{tBu})_3]$  and the study of its reactivity toward  $\text{H}_2$ . They showed that under  $\text{H}_2$  at  $150^\circ\text{C}$  the zirconium–carbon bonds of  $[(\text{tSiO})\text{Zr}(\text{CH}_2\text{tBu})_3]$  undergo hydrogenolysis to generate very reactive hydride intermediates such as  $[(\text{tSiO})\text{-ZrH}_3]$ , which further react with the silica surface to give  $[(\text{tSiO})_2\text{ZrH}_2]$  and  $[(\text{tSiO})_3\text{ZrH}]$  (Scheme 3) along with silicon hydrides. Indeed the  $^1\text{H}$  MAS and  $^1\text{H}$  2D DQ MAS spectra (Figure 7) performed on the gas-solid reaction products showed the presence of ZrH and  $\text{ZrH}_2$  species characterized by peaks at  $\delta = 10.1$  and  $12.1$  ppm with very different  $T_1$ , plus other signals due to SiH, SiR and SiOH groups. In the  $^1\text{H}$  2D DQ MAS spectrum a strong autocorrelation peak for the resonance at  $\delta = 12.1$  ppm ( $\delta = 24.2$  ppm in the  $\omega_1$  dimension), due to close proximity with protons of the same species, unambiguously allowed the resonance assignment to the  $\text{ZrH}_2$  group.

The  $[(\text{tSiO})_2\text{ZrH}_2]$  and  $[(\text{tSiO})_3\text{ZrH}]$  species were, then, reacted with  $\text{CO}_2$  and  $\text{N}_2\text{O}$  affording the corresponding formate  $[(\text{tSiO})_{4-x}\text{Zr}\{\text{O-C(=O)H}\}_x]$  and hydroxide complexes  $[(\text{tSiO})_{4-x}\text{Zr}(\text{OH})_x]$  (where  $x$  is 1 or 2) as major surface products.

Braga et al. have also presented an investigation of the reactivity of two different sandwich organometallic dicarboxylic acid compounds  $\{[\text{Co}^{\text{III}}(\eta^5\text{-C}_5\text{H}_4\text{COOH})(\eta^5\text{-C}_5\text{H}_4\text{COO})]\}$  and  $[\text{Fe}(\eta^5\text{-C}_5\text{H}_4\text{COOH})_2]\}$  toward volatile acids and bases.<sup>[11,91]</sup>

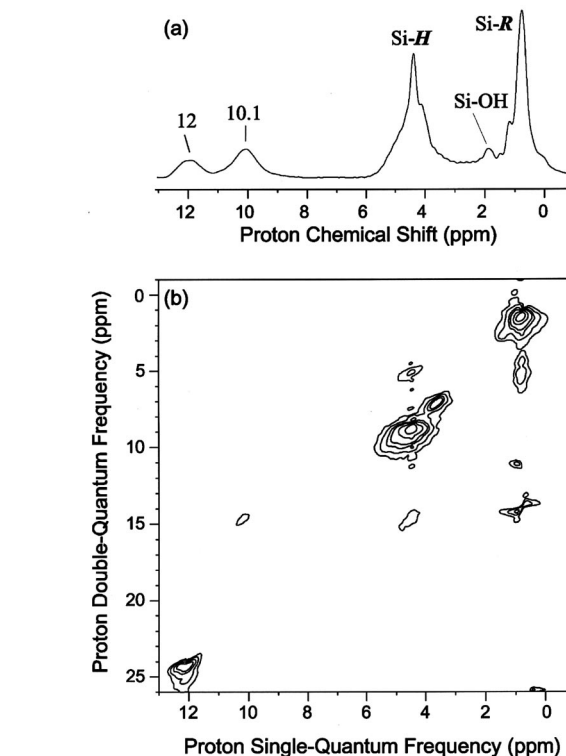
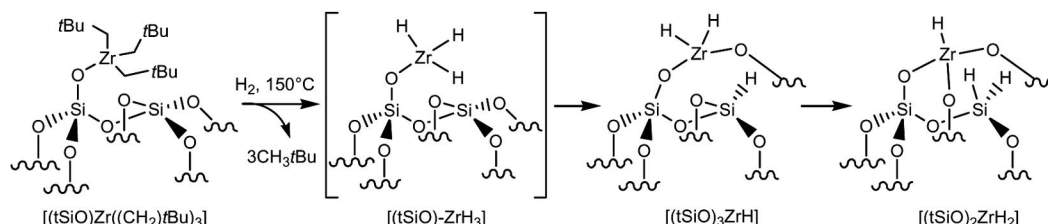


Figure 7. (a)  $^1\text{H}$  1D MAS NMR spectrum of  $[\text{Zr-H}]$  species obtained in the solid-state reaction between  $[(\text{tSiO})\text{Zr}(\text{CH}_2\text{tBu})_3]$  and  $\text{H}_2$  at  $150^\circ\text{C}$ . (b)  $^1\text{H}$  2D DQ MAS spectrum of  $[\text{Zr-H}]$  species.<sup>[90]</sup>

$\text{C}_5\text{H}_4\text{COO})]$  and  $[\text{Fe}(\eta^5\text{-C}_5\text{H}_4\text{COOH})_2]\}$  toward volatile acids and bases.<sup>[11,91]</sup>

The robust organometallic zwitterion  $[\text{Co}^{\text{III}}(\eta^5\text{-C}_5\text{H}_4\text{COOH})(\eta^5\text{-C}_5\text{H}_4\text{COO})]$  reversibly absorbs formic acid from vapours selectively forming a 1+1 co-crystal,  $[\text{Co}^{\text{III}}(\eta^5\text{-C}_5\text{H}_4\text{COOH})(\eta^5\text{-C}_5\text{H}_4\text{COO})][\text{HCOOH}]$  (Co-[HCOOH]) from which the zwitterion and the acid can be fully recovered by mild thermal treatment.<sup>[91]</sup> As shown in Figure 8, no proton transfer from formic acid to the deprotonated  $-\text{COO}_2$  group on the zwitterion crystalline is observed in Co-[HCOOH]. The process was investigated by  $^{13}\text{C}$  CPMAS NMR spectroscopy. The Figure 9 shows the comparison between NMR spectra of  $[\text{Co}^{\text{III}}(\eta^5\text{-C}_5\text{H}_4\text{COOH})(\eta^5\text{-C}_5\text{H}_4\text{COO})]$  and Co-[HCOOH]. The resonance at  $\delta = 164.4$  ppm is attributed to formic acid molecules. The presence of only one resonance for carboxylic carbon atoms of the zwitterion at  $\delta = 167.9$  ppm is indicative of proton exchange on the NMR time scale, between



Scheme 3.

donor and acceptor atoms along the O–H–O bond. These groups are “frozen out” as distinct  $\text{COO}^-$  and  $\text{COOH}$  units in the XRD experiment.

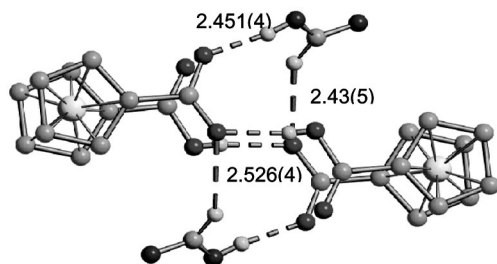


Figure 8. The dimers of  $[\text{Co}^{\text{III}}(\eta^5\text{-C}_5\text{H}_4\text{COOH})(\eta^5\text{-C}_5\text{H}_4\text{COO})]$  interact with two formic acid molecules via O–H $\cdots$ O HBs and C–H $\cdots$ O HBs.<sup>[91]</sup>

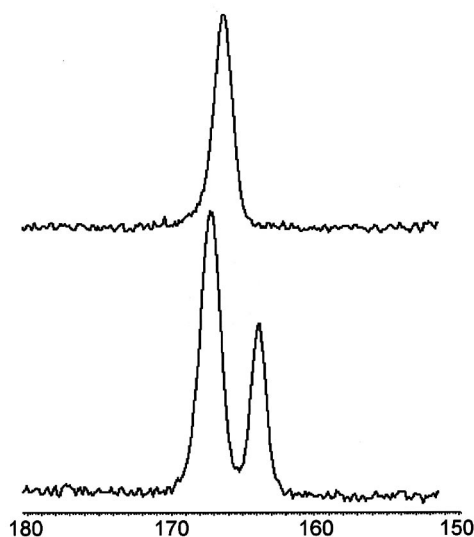


Figure 9.  $^{13}\text{C}$  CP-MAS NMR spectra of the solid  $[\text{Co}^{\text{III}}(\eta^5\text{-C}_5\text{H}_4\text{COOH})(\eta^5\text{-C}_5\text{H}_4\text{COO})]$  (top) and  $\text{Co}[\text{HCOOH}]$  (bottom) acquired at 8 kHz.<sup>[91]</sup>

On the other hand, two polymorphs of the compound  $[\text{Fe}(\eta^5\text{-C}_5\text{H}_4\text{COOH})_2]$ , (form I-monoclinic and form II-triclinic) have been employed in solid-gas reactions at room temperature with the gaseous bases  $\text{NH}_3$ ,  $\text{NH}_2(\text{CH}_3)$ , and  $\text{NH}(\text{CH}_3)_2$ .<sup>[11]</sup> The two crystal forms behave in exactly the same way in the solid-gas reaction, generating the same products, identified as the anhydrous crystalline salts  $[\text{NH}_4]_2[\text{Fe}(\eta^5\text{-C}_5\text{H}_4\text{COO})_2]$   $\{\text{Fe-NH}_4\}$ ,  $[\text{NH}_3\text{CH}_3]_2[\text{Fe}(\eta^5\text{-C}_5\text{H}_4\text{COO})_2]$   $\{\text{Fe-NH}_3\text{CH}_3\}$ , and  $[\text{NH}_2(\text{CH}_3)_2]_2[\text{Fe}(\eta^5\text{-C}_5\text{H}_4\text{COO})_2]$   $\{\text{Fe-NH}_2(\text{CH}_3)_2\}$ .

The comparison between powder diffractograms and between NMR spectra suggests very similar structures for these salts. Thus the chemical formula and crystal structure of  $\text{Fe-NH}_2(\text{CH}_3)_2$  (Figure 10) has been proposed also for compounds  $\text{Fe-NH}_4$  and  $\text{Fe-NH}_3\text{CH}_3$ , for which no single crystals could be obtained.

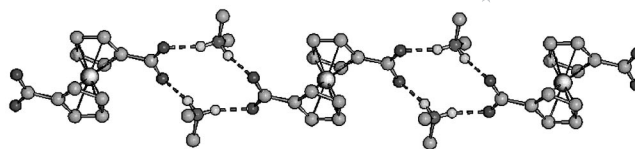


Figure 10. Packing arrangement of the salt  $[\text{NH}_2(\text{CH}_3)_2]_2[\text{Fe}(\eta^5\text{-C}_5\text{H}_4\text{COO})_2]$   $\{\text{Fe-NH}_2(\text{CH}_3)_2\}$  showing the  $^+\text{N-H}\cdots\text{O}^-$  interactions.<sup>[11]</sup>

Small shifts observed in the product spectra surmise the presence of similar hydrogen bonding framework and crystal packing interactions. Further information on the molecular structure were obtained by  $^{15}\text{N}$  CPMAS spectra characterized by a single resonance in the range 0.0 to  $-3.0$  ppm typical of an ammonium group.

Ammonia removal from  $\text{Fe-NH}_4$ , originating from either form I or form II, produces only the monoclinic form I, which is not the most thermodynamically stable of the two forms.

Interestingly forms I and II of  $[\text{Fe}(\eta^5\text{-C}_5\text{H}_4\text{COOH})_2]$  constitute a monotropic system (they do not interconvert via a solid-solid phase transition before melting): the ammonia absorption/release process, therefore, can be seen as a solid-state way to convert form II into form I. It is worth pointing out that the absorption/desorption process, in this case, implies a profound and dramatic *cis-trans* structural rearrangement also accompanied by the proton transfer processes detected by SS NMR spectroscopy.

### Solid-Solid Reactions

Concerning solid-solid reactivity, there has been great interest in finding mechanistic aspects in the context of intra- and inter-crystal reactions. Again, the crystal packing determines the extent of molecular loosening required for the molecules to reorient sufficiently to undergo molecular changes. Kaupp, by means of atomic force microscopy (AFM), has put forward a general mechanism involving three stages.<sup>[92]</sup> Thus considering a generic reaction  $\text{A} + \text{B} \rightarrow \text{C}$ : step (a) is the phase rebuilding, when there are directional long-range migrations of reactant molecules. This is driven by the internal pressure which comes from formation of C at the interface between A and B. It distorts the original crystal structures and results in the formation of crystal-correlated surface features (defects and mixed A–B–C phase). Step (b) is the phase transformation when the product lattice discontinuously forms and grows from the distorted mixed A–B–C phase. In step (c) the chemical and geometrical mismatch among A, B and C phases causes crystal disintegration with formation of new surfaces. This in turn reveals fresh surfaces of reactants allowing formation of a new distorted mixed A–B–C phase upon continued grinding. In addition to this description, Scott and co-workers have highlighted that often solvent-free reactions between solid reactants actually proceed through formation of eutectics between reactants and product(s) i.e. through formation of a liquid or melt phase containing an

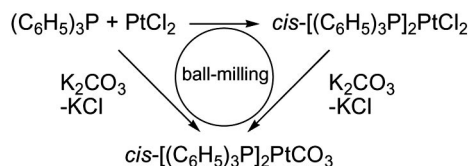


intimate mixture of macroscopic solid reactant particles; in this way molecules of the solid particles are sufficiently mobile for frequent molecular collisions to occur.<sup>[93]</sup> Thus these reactions should be classified as liquid/liquid or liquid/solid systems reacting without added solvents as confirmed also by other authors,<sup>[94,95]</sup> though each case has to be carefully evaluated and confirmed.

Usually, in solid-solid reactions, the solid-state NMR technique provides information on the reaction proceeding and on the product formation. Many examples are found in literature where the solid-state NMR has been used because of the possibility of clearly distinguish between the reactant and the product spectra.

For instance Pecharsky and co-workers used <sup>31</sup>P MAS NMR, combined with XRPD and DTA, for monitoring the formation of transition metal complexes,<sup>[96]</sup> phosphonium salts<sup>[95]</sup> and phosphorus ylides.<sup>[97]</sup>

They obtained the *cis*-[(Ph<sub>3</sub>P)<sub>2</sub>PtCl<sub>2</sub>] complex after ball-milling of polycrystalline PtCl<sub>2</sub> and Ph<sub>3</sub>P; then *cis*-[(Ph<sub>3</sub>P)<sub>2</sub>PtCO<sub>3</sub>] has been synthesised from *cis*-[(Ph<sub>3</sub>P)<sub>2</sub>PtCl<sub>2</sub>] with an excess of anhydrous K<sub>2</sub>CO<sub>3</sub> (Scheme 4). While the products exhibited an unidentifiable amorphous XRPD pattern, <sup>31</sup>P MAS resonances and Pt–P doublets (<sup>195</sup>Pt, natural abundance 33.8%), were in agreement with the formation of Pt–P bonds confirming the formation of the *cis*-[(Ph<sub>3</sub>P)<sub>2</sub>PtCl<sub>2</sub>] complex. The available experimental data suggested that mechanical processing enables interactions of reacting centres in the solid state by breaking firstly the crystallinity of the reactants and then by providing the mass transfer in the absence of a solvent.



Scheme 4.

The solid-state NMR technique has also provided valuable information about the HB interactions in a series of supramolecular complexes obtained by reacting the sandwich compound [Co<sup>III</sup>(η<sup>5</sup>-C<sub>5</sub>H<sub>4</sub>COOH)(η<sup>5</sup>-C<sub>5</sub>H<sub>4</sub>COO)] with a number of crystalline alkali salts MX (M = K<sup>+</sup>, Rb<sup>+</sup>, Cs<sup>+</sup>, NH<sub>4</sub><sup>+</sup>; X = Cl<sup>-</sup>, Br<sup>-</sup>, I<sup>-</sup>, PF<sub>6</sub><sup>-</sup>) by grinding or kneading, i.e. solid-state mixing in the presence of a catalytic amount of solvent, if necessary.<sup>[98]</sup> The mechanochemical reaction implied a profound solid-state rearrangement accompanied by breaking and reforming of O–H⋯O hydrogen-bonding interactions to afford supramolecular complexes of formula [Co<sup>III</sup>-(η<sup>5</sup>-C<sub>5</sub>H<sub>4</sub>COOH)(η<sup>5</sup>-C<sub>5</sub>H<sub>4</sub>COO)]<sub>2</sub>M<sup>+</sup>X<sup>-</sup> (Figure 11). By changing the salt, the similarity of the <sup>13</sup>C CPMAS spectra was in full agreement with identical packing, except for a lower frequency shift on descending the alkaline series. This shift has been related to the lengthening of the O⋯O HB that occurs by increasing the cation size inside the cage.

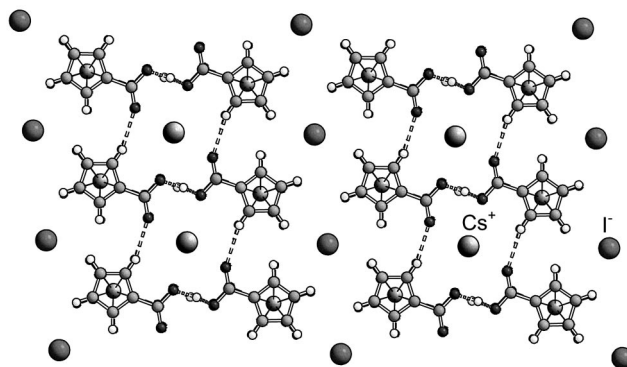


Figure 11. The structure of [Co<sup>III</sup>-(η<sup>5</sup>-C<sub>5</sub>H<sub>4</sub>COOH)(η<sup>5</sup>-C<sub>5</sub>H<sub>4</sub>COO)]<sub>2</sub>Cs<sup>+</sup>I<sup>-</sup> that evidences the encapsulation of Cs<sup>+</sup> ions within a cage formed by four zwitterionic molecules.<sup>[98]</sup>

The solid-state complexation of alkali cations by the organometallic zwitterion has been described as a special kind of solvation process taking place in the solid state.

The organometallic complex [Fe(η<sup>5</sup>-C<sub>5</sub>H<sub>4</sub>-C<sub>5</sub>H<sub>4</sub>N)<sub>2</sub>] has been reacted in the solid state with organic acids (anthranilic and pimelic) in order to obtain insights into the factors controlling the process. In the former case (organometallic complex-anthranilic acid) it has been found that the intermediacy of a catalytic amount of solvent or melting of one reactant is an essential condition for the occurrence of the reaction.<sup>[94]</sup> In the latter case (organometallic complex-pimelic acid) it has been observed that the protic or aprotic nature of the solvent used in vapour digestion experiments determined the stoichiometry of the products.<sup>[99]</sup>

The reaction of the organometallic complex [Fe(η<sup>5</sup>-C<sub>5</sub>H<sub>4</sub>-C<sub>5</sub>H<sub>4</sub>N)<sub>2</sub>] with the anthranilic acid (C<sub>6</sub>H<sub>4</sub>)NH<sub>2</sub>-COOH led to the hydrogen bonded supramolecular macrocycle {[Fe(η<sup>5</sup>-C<sub>5</sub>H<sub>4</sub>-C<sub>5</sub>H<sub>4</sub>N)<sub>2</sub>][(C<sub>6</sub>H<sub>4</sub>)NH<sub>2</sub>-COOH]}<sub>2</sub>.<sup>[94]</sup> The product has been fully characterized by means of XRPD, <sup>13</sup>C and <sup>15</sup>N CPMAS NMR and single crystal XRD. It has been shown that the same product can be quantitatively obtained by three different processes, namely kneading with MeOH, wet compression (i.e. pressure in the presence of MeOH without mixing) and “vapour digestion” (i.e. a mixture of the solid reactants is left in an atmosphere of MeOH vapours). The product can also be obtained via thermally induced reaction of a mixture of the two solid reactants, while no reaction is observed by dry mixing and dry compression. The NMR spectroscopic data were also useful in ascertaining the co-crystal nature of the adduct since no hydrogen transfer from the COOH group to the N pyridine has been detected by means of <sup>13</sup>C and <sup>15</sup>N CPMAS experiments.

Concerning the solid [Fe(η<sup>5</sup>-C<sub>5</sub>H<sub>4</sub>-C<sub>5</sub>H<sub>4</sub>N)<sub>2</sub>], the protic nature of the solvent used for the “vapour digestion” of the mixture ferrocenyl complex/pimelic acid HOOC(CH<sub>2</sub>)<sub>5</sub>-COOH determines the product chemical composition.<sup>[99]</sup> The 1:1 co-crystal was obtained by exposure to vapours of aprotic solvents, while the 1:2 co-crystal is formed only in presence of protic solvents. Other solid-state techniques have been tried (grinding and kneading), but no interconversions or co-crystal formation have been observed.



The structure has been obtained from single crystal XRD, while the salt or co-crystal nature of the products was ascertained by  $^{13}\text{C}$  COOH and  $^{15}\text{N}$  pyridine nitrogen chemical shifts. The analysis of the product allowed to afford some insight into the mechanism of the “vapour digestion”: the tiny amount of solvent adsorbed on the grains surface creates a “solution-like” environment between the contact surfaces wherein the reactants dissolve and the product immediately precipitate out.

### Solid-State Mobility vs. Solid-State Reactivity

Recent studies have demonstrated that molecular mobility is an important factor affecting the chemical stability of amorphous pharmaceuticals.<sup>[100]</sup> However, quantitative correlations between molecular mobility and chemical stability have not yet been elucidated.

It is widely accepted that low mobility in the glassy state due to a rather high viscosity renders chemical reactions difficult though the applicability of this generalization to different reactions is yet to be established. For instance conflicts exist on the role of glass transition phenomena (i.e. the decreased viscosity and an increased mobility above the glass transition temperature) on the rates of chemical reactions.<sup>[101]</sup>

Apart from the case cited above of the reaction of  $[\text{P}(\text{CH}_2\text{CH}_2\text{PPh}_2)_3\text{Co}(\text{N}_2)][\text{BPh}_4]$  with vapour of acetylene, ethylene, formaldehyde, acetaldehyde and carbon monoxide, in the transition metal complex literature there are only few unambiguous examples in which the mobility of a system may be correlate to its reactivity or at least where the mobility determines reaction pathways.

An example is the *cis-trans* isomerization of solid  $[(\eta^5\text{-C}_5\text{H}_5)\text{Fe}(\mu\text{-CO})(\text{CO})]_2$ .<sup>[102]</sup> A thorough analysis revealed that the process, known to take place in both directions in solution, occurs irreversibly (from *cis* to *trans*) in the solid state. The transformation, achieved by heating the sample

and monitored by  $^{13}\text{C}$  CPMAS, has been shown to obey a first-order Avrami–Erofe’ev rate law typical of a nucleation and growth mechanism. Notably, the observed irreversibility of this process was attributed to local differences of CO fluxional behaviour in both the *cis* and *trans* isomers. Indeed, the bridging-terminal carbonyl exchange mechanism in the *trans* form having a low  $E_a$ , i.e. CO ligand highly fluxional, is independent from the isomerization process. On the contrary, in the *cis* isomer it occurs only through the *cis-trans* isomerization because it requires an enantiomerization through a rotation about the Fe–Fe bond by  $2\pi/3$  or  $4\pi/3$ , which requires a higher  $E_a$ .

Another example concerns the increased mobility with respect to the crystalline molecule of (1–4,4a,8b- $\eta^6$ -biphenylene)tricarbonylchromium complex supported on silica gel which leads to an increased instability.<sup>[103]</sup> Indeed, the  $^{13}\text{C}$  CPMAS data of the crystalline compound confirm that in the solid state at room temperature the rotation of the  $\text{Cr}(\text{CO})_3$ -group around the Cr–ligand axis stops. On the other hand the  $^{13}\text{C}$  MAS spectrum of the complex supported on silica gel is completely resolved showing very narrow signals ( $< 15$  Hz) indicating a considerable mobility of the absorbed molecules able to average the strong dipolar interaction. The authors observed also that (1–4,4a,8b- $\eta^6$ -biphenylene)tricarbonylchromium complex has intermediate stability when supported on silica gel. Indeed, qualitative kinetic data of such decomposition obtained by means of NMR show a gradual decomposition at room temperature to form biphenylene and  $\text{Cr}(\text{CO})_6$  after 24 h (Figure 12).

The solid-gas reactions of the “lightly stabilized”  $[\text{Os}_3(\text{CO})_{11}\text{X}]$  clusters ( $\text{X} = \text{NCCH}_3$ ,  $\text{C}_2\text{H}_4$ ) with gaseous reactants ( $\text{CO}$ ,  $\text{NH}_3$ , and  $\text{H}_2$ ) represents a case where the ligand fluxionality determines the stereochemistry of the reactions and where, by looking at the  $^{13}\text{C}$  MAS and  $^{15}\text{N}$  CPMAS spectra, it has been possible to understand it.<sup>[104]</sup> The  $[\text{Os}_3(\text{CO})_{11}\text{X}]$  complexes ( $\text{X} = \text{NCCH}_3$ ,  $\text{C}_2\text{H}_4$ ) undergo

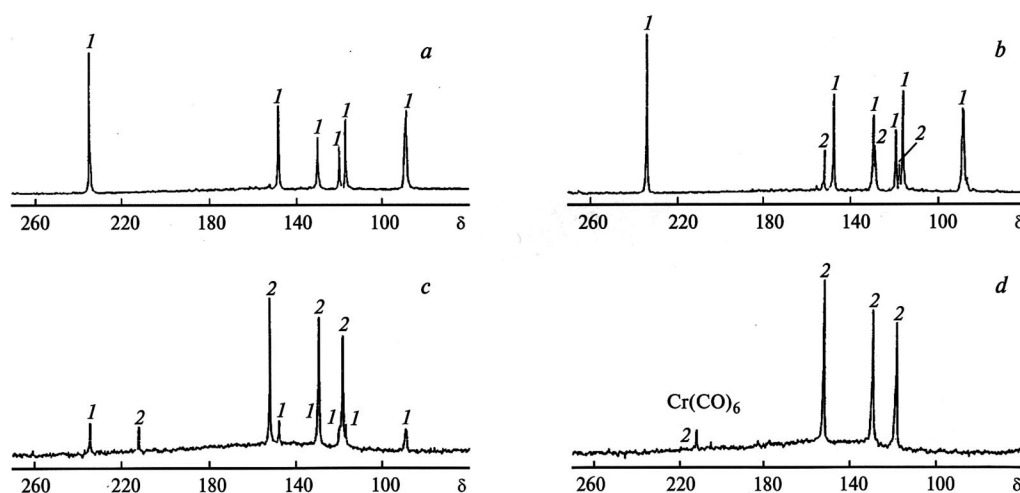


Figure 12.  $^{13}\text{C}$  MAS NMR spectra of a (1–4,4a,8b- $\eta^6$ -biphenylene)tricarbonylchromium complex applied onto silica gel (a) and kinetics of its decomposition after keeping at 25 °C for 4 (b), 12 (c), and 24 h (d); (1) signals of the complex; (2) signals of the biphenylene ligand and  $\text{Cr}(\text{CO})_6$ .<sup>[103]</sup>

substitution of the axially bound acetonitrile ligand and the equatorially coordinated ethene ligand by gaseous reactants. For the reaction with  $^{13}\text{CO}$  to form  $[\text{Os}_3(\text{CO})_{11}(^{13}\text{CO})]$  no site selectivity has been observed. Indeed its  $^{13}\text{C}$  MAS NMR spectrum shows that the  $^{13}\text{CO}$  ligand is equally distributed over axial (ax) and equatorial (eq) sites as observed by the integration of the two regions assigned to axial (from 188 to 180 ppm) and equatorial (from 175 to 167 ppm) carbonyls, respectively (Figure 13).

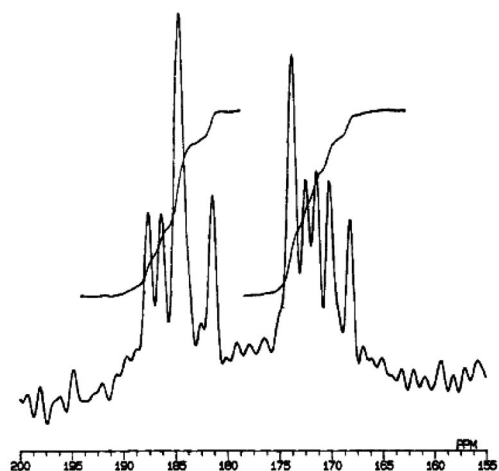


Figure 13. Isotropic region of the  $^{13}\text{C}$  MAS spectrum (spinning speed 6 kHz, recycle time 120 s, r.t.) of  $\{\text{Os}_3(\text{CO})_{11}(^{13}\text{CO})\}$  obtained by the solid-gas reaction of  $[\text{Os}_3(\text{CO})_{11}(\text{NCCH}_3)]$  with  $^{13}\text{CO}$ .<sup>[104]</sup>

The random distribution of  $^{13}\text{CO}$  over axial and equatorial sites indicates that fluxional behaviour occurs at some stage during the reaction.

On the contrary in the reaction with  $\text{NH}_3$ , the ammonia ligand results coordinated in an axial position to afford  $[\text{Os}_3(\text{CO})_{11}(\text{NH}_3)]$ , as deduced by the presence of a single resonance in the  $^{15}\text{N}$  CPMAS spectrum. Two interpretations have been proposed: (i)  $\{\text{Os}_3(\text{CO})_{11}\}$  reacts with ammonia only when the vacant coordination site is in an axial position (kinetically controlled reaction), or (ii) both the ax and eq isomers are formed, but the less stable equatorial one rearranges quickly to give the axial isomer (thermodynamically controlled reaction).

The observed stereochemistry of the reaction products of  $[\text{Os}_3(\text{CO})_{11}\text{X}]$  with  $\text{CO}$  and  $\text{NH}_3$  suggested the presence of a coordinatively unsaturated intermediate  $\{\text{Os}_3(\text{CO})_{11}\}$ , which is formed upon release of the acetonitrile/ethene ligand (dissociative reaction pathway) and which displays an intramolecular axial-equatorial exchange of the vacant coordination site.

To best of our knowledge in the literature there are no other clear examples able to elucidate what is the role of molecular dynamics in determining the reactivity leaving the question unanswered: however, as often as not, this it has not even considered some time because they focused only on the reactivity some time because they focused only on the mobility.

## Conclusions and Perspectives

Solid-state mobility and solid-state reactivity involving transition metal complexes are becoming increasingly important for the possibilities offered by a topochemical control in solid reactions and for their implications in the green chemistry. Transition metal complexes represent an unlimited source of solid-state dynamic processes due to the presence of highly mobile groups such as hydrides,  $\pi$ -bonded ligands, or ligands such  $\text{CO}$  or phosphane, all having different coordination modes (terminal,  $\mu_2$ -bridging,  $\mu_3$ -bridging etc.). Furthermore the presence of lightly stabilized ligands and the possibility of expanding the coordination sphere open numerous perspectives in the solid-solid and the solid-gas reactivity.

Among a large array of possible techniques, solid-state NMR is one of the more versatile tool for studying dynamics in a solid and the interest in the solid-state NMR techniques for investigating solid-state reactions is growing since: a) several parameters such as lineshape and shielding, dipolar and quadrupolar tensors are temperature dependent; b) activation energies of dynamic processes can be determined by spin-lattice ( $T_1$ ) relaxation of individual atoms using variable temperature experiments; c) orientation of the rotation axes can be carefully calculated from the analysis of chemical shift anisotropy or quadrupolar spinning sideband manifolds; d) dynamic mechanisms can be understood at molecular level on the basis of the coalescence of solid-state NMR resonances using variable temperature experiments; e) intermediate species can be detected and fully characterized by a complete resonance assignment through spectral editing experiments; f) powder samples can be in principle fully characterized; g) kinetics and mechanisms can be followed and elucidated.

The key question at the end of this microreview is: what is the molecular dynamic role in determining solid-state reactivity in transition metal complexes?

Unfortunately it is not trivial to find an exhaustive answer. By comparing the massive literature concerning ligand mobility and the relatively few examples of solid-state reactivity an evident influence of mobility on the reactivity cannot be demonstrated, in part due to limitations of earlier experimental designs. This has to be compared with a relevant studies in organic systems where the relationship between mobility and reactivity has been investigated.<sup>[105]</sup> In particular crystalline molecular machines combine often controllable chemical processes and dynamics. Amphidynamic crystals specifically designed with static and mobile parts capable of responding to the presence of external stimuli have been proposed.<sup>[106]</sup>

However, it seems that quantitative correlations between molecular mobility and chemical stability have not yet been fully elucidated underlining the necessity of much more efforts in that direction. It is surprising that in the case of transition metal complex field which, as stated above, presents a plethora of dynamic and fluxional systems, only few clear examples can be found.

In order to explain the reason for this lack of correlation between mobility and reactivity involving transition metal complexes it is important to stress that the motion of the ligands in transition metal complexes involves equivalent sites or occurs without disruption of the crystal lattice. Also, by considering that the moving molecules are completely isolated from the surrounding environment and single-crystal-to-single-crystal transformation are quite rare, it seems not so surprising that the solid-state mobility is more strictly related to the formation of a new crystal phase (polymorphism) than the formation or breakage of covalent bonds. Furthermore molecular and supramolecular systems that undergo collective movements have been markedly less studied in transition metal chemistry.

We believe that such perspectives, the outgoing improvements of new solid-state NMR techniques in studying solid-state dynamic and reactivity, the comprehensive example collection here reported and present in literature, will stimulate further scientific efforts in the field of transition metal complexes. Indeed, further works may afford new insights able to elucidate this controversial subject that seems to embrace not only the organometallic chemistry but also organic, pharmaceutical, polymer and food fields.

## Acknowledgments

We thank the Italian Ministero dell'Istruzione, dell'Università e della Ricerca (MIUR), (Prin 2006035198\_004) for the financial support. We thank Dr. Nadia Garino, Dr. Luca Pellegrino and all students involved in the research and development of the projects described above over the past several years.

- [1] V. Balzani, M. Venturi, A. Credi, *Molecular Devices and Machines*, Wiley-VCH, Weinheim, **2003**.
- [2] a) E. Katz, O. Lioubashevsky, I. Wilner, *J. Am. Chem. Soc.* **2004**, *126*, 15520–15532; b) A. Harada, *Acc. Chem. Res.* **2001**, *34*, 456–464.
- [3] a) T. S. Piper, G. Wilkinson, *J. Inorg. Nucl. Chem.* **1956**, *3*, 32; b) T. S. Piper, G. Wilkinson, *J. Inorg. Nucl. Chem.* **1956**, *3*, 104–124.
- [4] T. A. Albright, *Acc. Chem. Res.* **1982**, *15*, 149–155.
- [5] D. Braga, *Chem. Rev.* **1992**, *92*, 633–665.
- [6] K. G. Orrell, *Ann. Rep. NMR Spectrosc.* **1999**, *37*, 1–74.
- [7] B. E. Mann, *Spectroscopic Properties Inorganic and Organometallic Compounds* (Ed.: G. Davidson), Royal Society of Chemistry, Cambridge, **1997**, vol. 30, pp. 1–209.
- [8] C. Bianchini, M. Peruzzini, F. Zanobini, *Organometallics* **1991**, *10*, 3415–3417.
- [9] a) S. R. Byrn, R. R. Pfeiffer, J. G. Stowell, *Solid-state chemistry of drugs*, 2nd ed., West Lafayette, SSCI, Inc., **1999**; b) J. T. Carstensen, *Drug stability: principle and practice*, 2nd ed., New York: Marcel Dekker, Inc. **1995**; c) I. C. Paul, D. Y. Curtin, *Acc. Chem. Res.* **1973**, *6*, 217–225; d) B. C. Hancock, G. Zograf, *J. Pharm. Sci.* **1997**, *86*, 1–12; e) E. Y. Shalae, G. Zograf, *J. Pharm. Sci.* **1996**, *85*, 1137–1141; f) E. R. Oberholzer, G. S. Brenner, *J. Pharm. Sci.* **1979**, *68*, 836–866; g) M. J. Pikal, K. M. Dellerman, *Int. J. Pharm.* **1989**, *50*, 233–252.
- [10] S. L. Shamblin, B. C. Hancock, M. J. Pikal, *Pharm. Res.* **2006**, *23*, 2254–2268.
- [11] D. Braga, F. Grepioni, M. Polito, M. R. Chierotti, S. Ellena, R. Gobetto, *Organometallics* **2006**, *25*, 4627–4633.
- [12] M. R. Chierotti, R. Gobetto, L. Pellegrino, L. Milone, P. Venturello, *Cryst. Growth Des.* **2008**, *8*, 1454–1457.
- [13] K. J. D. MacKenzie, M. E. Smith, *Multinuclear Solid State NMR of Inorganic Materials*, Pergamon Materials Series, vol. 6, Pergamon–Elsevier, Oxford, **2002**.
- [14] A. Gavezzotti, *Nouv. J. Chim.* **1982**, *6*, 443–450.
- [15] C. Job, J. Zajicek, M. F. Brown, *Rev. Sci. Instrum.* **1996**, *67*, 2113–2122.
- [16] D. Allion, C. P. Slichter, *Phys. Rev. Lett.* **1964**, *12*, 168–171.
- [17] K. Schmidt-Rohr, H. W. Spiess, *Multidimensional Nuclear Magnetic Resonance and Polymers*, Academic Press, London, **1994**.
- [18] J. R. Lyster, *High-Resolution NMR of Glassy Amorphous Polymers, Methods in Stereochemical Analysis, High Resolution NMR Spectroscopy of Synthetic Polymers in Bulk* (Ed.: R. A. Komoroski), VCH Publishers, Deerfield Beach, **1986**, vol. 7, p. 63.
- [19] G. L. Hoatson, R. L. Vold, *NMR: Basic Princ. Prog.* **1994**, *32*, 1–67.
- [20] J. H. Davis, K. R. Jeffrey, M. J. Bloom, T. Valic, P. Higgs, *Chem. Phys. Lett.* **1976**, *42*, 390–394.
- [21] L. Frydman, S. Vallabhaneni, Y. K. Lee, M. Emsley, *J. Chem. Phys.* **1994**, *101*, 111–117.
- [22] W. P. Rothwell, J. S. Waugh, *J. Chem. Phys.* **1981**, *74*, 2721–2732.
- [23] D. H. T. Edzes, J. P. C. Bernards, *J. Am. Chem. Soc.* **1984**, *106*, 1515–1517.
- [24] a) M. J. Duer (Ed.), *Solid State NMR Spectroscopy: Principles and Applications*, Blackwell, Oxford, **2002**; b) M. J. Duer, *Ann. Rep. NMR Spectrosc.* **2006**, *59*, 41–116.
- [25] a) S. P. Brown, H. W. Spiess, *Chem. Rev.* **2001**, *101*, 4125–4155; b) K. D. M. Harris, E. Y. Cheung, *Chem. Soc. Rev.* **2004**, *33*, 526–538.
- [26] a) R. Gobetto, C. Nervi, E. Valfré, M. R. Chierotti, D. Braga, L. Maini, F. Grepioni, R. K. Harris, P. Y. Ghi, *Chem. Mater.* **2005**, *17*, 1457–1466; b) R. Giustetto, F. X. Llabrés i. Xamena, G. Ricchiardi, S. Bordiga, A. Damin, R. Gobetto, M. R. Chierotti, *J. Phys. Chem. B* **2005**, *109*, 19360–19368.
- [27] *Solid State Chemistry Techniques* (Ed.: A. K. Cheetham), Oxford University Press, Oxford, **1987**.
- [28] D. Braga, F. Grepioni, *Chem. Soc. Rev.* **2000**, *29*, 229–238.
- [29] K. J. D. MacKenzie, *Solid State Ionics* **2004**, *172*, 383–388.
- [30] R. K. Harris, *The Analyst* **2006**, *131*, 351–373.
- [31] M. R. Chierotti, R. Gobetto, *Chem. Commun.* **2008**, 1621–1634.
- [32] a) S. P. Brown, *Prog. Nucl. Magn. Reson. Spectrosc.* **2007**, *50*, 199–251; b) R. Gobetto, C. Nervi, M. R. Chierotti, D. Braga, L. Maini, F. Grepioni, R. K. Harris, P. Hodgkinson, *Chem. Eur. J.* **2005**, *11*, 7461–7471.
- [33] R. K. Harris, *Solid State Sci.* **2004**, *6*, 1025–1037.
- [34] D. Braga, L. Maini, C. Fagnano, P. Taddei, M. R. Chierotti, R. Gobetto, *Chem. Eur. J.* **2007**, *13*, 1222–1230.
- [35] a) J. Williams, A. McDermott, *J. Chem. Phys.* **1993**, *97*, 12393–12398; b) L. Zheng, K. W. Fishbein, J. Herzfeld, *J. Am. Chem. Soc.* **1993**, *115*, 6254–6261; c) D. Braga, L. Maini, G. de Sanctis, K. Rubini, F. Grepioni, M. R. Chierotti, R. Gobetto, *Chem. Eur. J.* **2003**, *9*, 5538–5548.
- [36] a) J. Brus, A. Jegorov, *J. Phys. Chem. A* **2004**, *108*, 3955–3964; b) I. Schnell, S. P. Brown, H. Yee Low, H. Ishida, H. W. Spiess, *J. Am. Chem. Soc.* **1998**, *120*, 11784–11795; c) D. Braga, G. Palladino, M. Polito, K. Rubini, F. Grepioni, M. R. Chierotti, R. Gobetto, *Chem. Eur. J.* **2008**, *14*, 10149–10159.
- [37] J. Brus, J. Jakes, *Solid State Nucl. Magn. Reson.* **2005**, *27*, 180–191.
- [38] S. A. Nierkoetter, C. E. Barnes, G. L. Garner, L. G. Butler, *J. Am. Chem. Soc.* **1994**, *116*, 7445–7446.
- [39] S. E. Anderson, *J. Organomet. Chem.* **1974**, *71*, 263–269.
- [40] a) C. H. Holm, J. A. Ibers, *J. Chem. Phys.* **1959**, *30*, 885–888; b) A. J. Campbell, C. A. Fyfe, D. Harold-Smith, K. R. Jeffrey, *Mol. Cryst. Liq. Cryst.* **1981**, *36*, 1–23.
- [41] I. S. Butler, P. J. Fitzpatrick, D. F. R. Gilson, G. Gomez, A. Shaver, *Mol. Cryst. Liq. Cryst.* **1981**, *71*, 213–218.



- [42] D. F. R. Gilson, G. Gomez, I. S. Butler, P. J. Fitzpatrick, *Can. J. Chem.* **1983**, *61*, 737–742.
- [43] A. E. Aliev, K. D. M. Harris, F. Guillaume, *J. Phys. Chem.* **1995**, *99*, 1156–1165.
- [44] D. O'Hare, S. J. Heyes, S. Barlow, S. Mason, *J. Chem. Soc., Dalton Trans.* **1996**, 2989–2993.
- [45] a) G. C. Campbell, F. A. Cotton, J. F. Haw, W. Schwotzer, *Organometallics* **1986**, *5*, 274–279; b) H. Heise, F. H. Kohler, M. Herker, W. Hiller, *J. Am. Chem. Soc.* **2002**, *124*, 10823–10832.
- [46] S. Aime, D. Braga, L. Cordero, R. Gobetto, F. Grepioni, S. Righi, S. Sostero, *Inorg. Chem.* **1992**, *31*, 3054–3059.
- [47] a) S. J. Heyes, M. A. Gallup, B. F. G. Johnson, J. Lewis, C. M. Dobson, *Inorg. Chem.* **1991**, *30*, 3850–3856; b) D. Braga, F. Grepioni, B. F. G. Johnson, J. Lewis, M. Martinelli, *J. Chem. Soc., Dalton Trans.* **1990**, 1847–1852; c) M. A. Gallop, B. F. G. Johnson, J. Keeler, J. Lewis, S. J. Heyes, C. M. Dobson, *J. Am. Chem. Soc.* **1992**, *114*, 2510–2520.
- [48] M. R. Chierotti, L. Garlaschelli, R. Gobetto, C. Nervi, G. Peli, A. Sironi, R. Della Pergola, *Eur. J. Inorg. Chem.* **2007**, 3477–3483.
- [49] A. M. Orendt, J. C. Facelli, Y. J. Jiang, D. M. Grant, *J. Phys. Chem. A* **1998**, *102*, 7692–7697.
- [50] A. Y. H. Lo, T. E. Bitterwolf, C. L. B. Macdonald, R. W. Schurko, *J. Phys. Chem. A* **2005**, *109*, 7073–7087.
- [51] A. J. Edwards, N. J. Burke, C. M. Dobson, K. Prout, S. J. Heyes, *J. Am. Chem. Soc.* **1995**, *117*, 4637–4653.
- [52] D. F. Brougham, P. J. Barrie, G. E. Hawkes, I. Abrahams, M. Motevalli, D. A. Brown, G. J. Long, *Inorg. Chem.* **1996**, *35*, 5595–5602.
- [53] E. J. Munson, M. C. Douskey, S. M. De Paul, M. Ziegeweid, L. Phillips, F. Separovic, M. R. Davies, M. J. Aroney, *J. Organomet. Chem.* **1999**, *577*, 19–23.
- [54] J. M. Lopez del Amo, G. Buntkowsky, H.-H. Limbach, I. Resa, R. Fernandez, E. Carmona, *J. Phys. Chem. A* **2008**, *112*, 3557–3565.
- [55] see for example R. L. Corey, T. M. Ivancic, D. T. Shane, E. A. Carl, R. C. Bowman, J. M. Bellosta von Colbe, M. Dornheim, R. Bormann, J. Huot, R. Zidan, A. C. Stowe, M. S. Conradi, *J. Phys. Chem. C* **2008**, *112*, 19784–19790, and references cited therein.
- [56] S. Aime, R. Gobetto, A. Orlandi, G. J. Goombridge, G. E. Hawkes, M. D. Mantle, R. D. Sales, *Organometallics* **1994**, *13*, 2375–2379.
- [57] R. A. Harding, H. Nakajama, T. Eguchi, N. Nakamura, B. T. Heaton, A. K. Smith, *Polyhedron* **1998**, *17*, 2857–2863.
- [58] G. Buntkowsky, H.-H. Limbach, *J. Low Temp. Phys.* **2006**, *143*, 55–114.
- [59] T. H. Walter, L. Reven, E. Oldfield, *J. Phys. Chem.* **1989**, *93*, 1320–1326.
- [60] C. E. Hanson, R. E. Benfields, A. W. Bott, B. F. G. Johnson, D. Braga, E. A. Marseglia, *J. Chem. Soc., Chem. Commun.* **1988**, 889–891.
- [61] S. J. Heyes, M. L. H. Green, C. M. Dobson, *Inorg. Chem.* **1991**, *30*, 1930–1937.
- [62] G. M. Bernard, R. E. Wasylshen, *Unusual Structures and Physical Properties in Organometallic Chemistry* (Eds.: M. Gielen, R. Willem, B. Wrackmeyer), John Wiley & Sons, **2002**, vol. 3, pp. 165–205.
- [63] R. Warmuth, *J. Incl. Phenom. Macrocycl. Chem.* **2000**, *37*, 1–38, and ref. therein.
- [64] F. Imashiro, D. Kuwawara, N. Kitazaki, T. Terao, *Magn. Reson. Chem.* **1992**, *30*, 796–797.
- [65] H. C. Canuto, S. J. Heyes, S. Aime, R. Gobetto, F. Napolitano, *J. Chem. Soc., Dalton Trans.* **2000**, 4075–4077.
- [66] S. Aime, H. C. Canuto, R. Gobetto, F. Napolitano, *Chem. Commun.* **1999**, 281–282.
- [67] S. Aime, M. R. Chierotti, R. Gobetto, A. Masic, F. Napolitano, H. C. Canuto, S. J. Heyes, *Eur. J. Inorg. Chem.* **2008**, 152–157.
- [68] a) R. P. Rastogi, P. S. Bassi, S. L. Chadha, *J. Phys. Chem.* **1963**, *67*, 2569–2573; b) A. O. Patil, D. Y. Curtin, I. C. Paul, *J. Am. Chem. Soc.* **1984**, *106*, 348–353; c) J. Fernandez-Bertran, J. C. Alvarez, E. Reguera, *Solid State Ionics* **1998**, *106*, 129–135; d) N. Shan, F. Toda, W. Jones, *Chem. Commun.* **2002**, 2372–2373; e) S. Nakamatsu, S. Toyota, W. Jones, F. Toda, *Chem. Commun.* **2005**, 3808–3810; f) K. Tanaka, F. Toda, *Chem. Rev.* **2000**, *100*, 1025–1074; g) D. Braga, F. Grepioni, *Angew. Chem. Int. Ed.* **2004**, *43*, 4002–4011; h) G. Kaupp, *Topics in Current Chemistry* (Ed.: F. Toda), Springer, Berlin, **2005**, *254*, pp. 95–183; i) D. W. Brice, D. O'Hare, *Inorganic Material*, John Wiley & Sons, New York, **1992**; j) M. Gielen, R. Willen, B. Wrackmeyer, *Solid State Organometallic Chemistry, Methods and Applications*, John Wiley & Sons, New York, **1999**.
- [69] a) G. R. Desiraju, *Crystal Engineering: The Design of Organic Solids*, Elsevier, Amsterdam, **1989**; b) M. D. Hollingsworth, *Science* **2002**, *295*, 2410–2413; c) D. Braga, F. Grepioni, G. R. Desiraju, *Chem. Rev.* **1998**, *98*, 1375–1405; d) D. Braga, G. R. Desiraju, J. Miller, A. G. Orpen, S. Price, *CrystEngComm* **2002**, *4*, 500–509; e) D. Braga, L. Brammer, N. Champness, *CrystEngComm* **2005**, *7*, 1–19.
- [70] a) M. Ogawa, T. Hashizume, K. Kuroda, C. Kato, *Inorg. Chem.* **1991**, *30*, 584–585; b) J. M. Thomas, R. Raja, G. Sankar, B. F. G. Johnson, D. W. Lewis, *Chem. Eur. J.* **2001**, *7*, 2973–2978; c) P. J. Nichols, C. L. Raston, J. W. Steed, *Chem. Commun.* **2001**, 1062–1063; d) R. Kuroda, Y. Imal, T. Sato, *Chirality* **2001**, *13*, 588–594; e) S. Apel, M. Lennartz, L. R. Nassimbeni, E. Weber, *Chem. Eur. J.* **2002**, *8*, 3678–3686; f) L. R. Nassimbeni, *CrystEngComm* **2003**, *5*, 200–203.
- [71] a) M. C. Etter, *J. Phys. Chem.* **1991**, *95*, 4601–4610; b) M. C. Etter, S. M. Reutzel, C. G. Choo, *J. Am. Chem. Soc.* **1993**, *115*, 4411–4412; c) W. H. Ojala, M. C. Etter, *J. Am. Chem. Soc.* **1992**, *114*, 10228–10293; d) V. R. Pedireddi, W. Jones, A. P. Chortlort, R. Docherty, *Chem. Commun.* **1996**, 987–988; e) A. V. Trask, W. D. S. Motherwell, W. Jones, *Chem. Commun.* **2004**, 890–891.
- [72] a) D. Braga, M. Curzi, A. Johansson, M. Polito, K. Rubini, F. Grepioni, *Angew. Chem. Int. Ed.* **2006**, *45*, 142–146; b) A. Pichon, A. Lazuen-Garay, S. L. James, *CrystEngComm* **2006**, *8*, 211–214; c) D. Braga, S. L. Giaffreda, F. Grepioni, A. Pettersen, L. Maini, M. Curzi, M. Polito, *Dalton Trans.* **2006**, 1249–1263.
- [73] a) D. Braga, M. Curzi, M. Lusi, F. Grepioni, *CrystEngComm* **2005**, *7*, 276–278; b) A. V. Trask, D. A. Haynes, W. D. S. Motherwell, W. Jones, *Chem. Commun.* **2006**, 51–53.
- [74] A. Lazuen Garay, A. Pichon, S. L. James, *Chem. Soc. Rev.* **2007**, *36*, 846–855.
- [75] C. Suryanarayana, *Prog. Mater. Sci.* **2001**, *46*, 1–184.
- [76] J. M. Thomas, S. E. Morsi, J. P. Desvergne, *Adv. Phys. Org. Chem.* **1978**, *15*, 63–151.
- [77] a) G. Kaupp, *Curr. Opin. Solid State Mater. Sci.* **2002**, *6*, 131–138; b) Q. Chu, D. C. Swenson, L. R. MacGillivray, *Angew. Chem. Int. Ed.* **2005**, *44*, 3569–3572, and ref. therein; c) N. L. Toh, M. Nagarathinam, J. J. Vittal, *Angew. Chem. Int. Ed.* **2005**, *44*, 2237–2241; d) G. S. Papaefstathiou, Z. Zhong, L. Geng, L. R. MacGillivray, *J. Am. Chem. Soc.* **2004**, *126*, 9158–9159.
- [78] H. Nakanishi, W. Jones, J. M. Thomas, M. B. Hursthouse, M. Motevalli, *J. Phys. Chem.* **1981**, *85*, 3636–3642.
- [79] K. Tanaka, T. Hiratsuka, S. Ohba, M. R. Naimi-Jamal, G. Kaupp, *J. Phys. Org. Chem.* **2003**, *16*, 905–912.
- [80] D. Braga, F. Grepioni, *Crystal Design, Structure and Function. Perspectives in Supramolecular Chemistry*, vol. 7 (Ed.: G. R. Desiraju), Wiley, Chichester, **2003**.
- [81] a) C. Bianchini, M. Peruzzini, A. Vacca, F. Zanobini, *Organometallics* **1991**, *10*, 3697–3707; b) C. Bianchini, C. Mealli, M. Peruzzini, F. Zanobini, *J. Am. Chem. Soc.* **1992**, *114*, 5905–5906; c) C. Bianchini, E. Farnetti, M. Graziani, J. Kaspar, F. Vizza, *J. Am. Chem. Soc.* **1993**, *115*, 1753–1759; d) A. R. Siedle, R. A. Newmark, *Organometallics* **1989**, *8*, 1442–1450; e) A. R. Siedle, R. A. Newmark, *J. Am. Chem. Soc.* **1989**, *111*, 2058–2062; f) A. R. Siedle, R. A. Newmark, M. R. V. Sahyun, P. A.



- Lyon, S. L. Hunt, R. P. Skarjune, *J. Am. Chem. Soc.* **1989**, *111*, 8346–8350.
- [82] a) J. A. N. Ajiou, S. L. Scott, *Organometallics* **1997**, *16*, 86–92; b) E. Le Roux, M. Chabanas, A. Baudouin, A. de Mallmann, C. Copéret, E. A. Quadrelli, J. Thivolle-Cazat, J.-M. Basset, W. Lukens, A. Lesage, L. Emsley, G. J. Sunley, *J. Am. Chem. Soc.* **2004**, *126*, 13391–13399.
- [83] C. Bianchini, F. Zanobini, S. Aime, R. Gobetto, R. Pisaro, L. Sordellis, *Organometallics* **1993**, *12*, 4757–4763.
- [84] a) C. Bianchini, C. Mealli, S. Midollini, L. Sacconi, *Inorg. Chim. Acta* **1978**, *31*, L433–L434; b) C. Bianchini, C. Mealli, A. Meli, L. Sacconi, *Inorg. Chim. Acta* **1980**, *43*, 223–228; c) K. D. Tau, R. Uriarte, T. J. Mazanec, D. W. Meek, *J. Am. Chem. Soc.* **1979**, *101*, 6614–6619; d) A. L. Balch, E. Y. Fung, *Inorg. Chem.* **1990**, *29*, 4764–4768.
- [85] a) A. J. Arce, M. R. Chierotti, Y. De Sanctis, A. J. Deeming, R. Gobetto, *Inorg. Chim. Acta* **2004**, *357*, 3799–3802; b) A. J. Arce, M. Chierotti, Y. De Sanctis, R. Gobetto, T. González, R. Machado, M. Márquez, *Inorg. Chim. Acta* **2009**, *362*, 291–294.
- [86] S. Aime, W. Dastrù, R. Gobetto, A. J. Arce, *Organometallics* **1994**, *13*, 4232–4236.
- [87] a) D. G. H. Ballard, *Adv. Catal.* **1973**, *23*, 263–325; b) Y. I. Yermakov, B. N. Kuznetsov, V. A. Zakharov, *Stud. Surf. Sci. Catal.* **1981**, *8*, 522; c) J. M. Basset, A. Choplin, *J. Mol. Catal.* **1983**, *21*, 95–108; d) C. Copéret, M. Chabanas, R. Petroff Saint-Arroman, J.-M. Basset, *Angew. Chem. Int. Ed.* **2003**, *42*, 156–181; e) S. L. Scott, J. M. Basset, G. P. Niccolai, C. C. Santini, J. P. Candy, C. Lecuyer, F. Quignard, A. Choplin, *New J. Chem.* **1994**, *18*, 115–122.
- [88] a) R. Petroff Saint-Arroman, M. Chabanas, A. Baudouin, C. Copéret, J.-M. Basset, A. Lesage, L. Emsley, *J. Am. Chem. Soc.* **2001**, *123*, 3820–3821; b) M. Chabanas, E. A. Quadrelli, B. Fenet, C. Copéret, J. Thivolle-Cazat, J.-M. Basset, A. Lesage, L. Emsley, *Angew. Chem. Int. Ed.* **2001**, *40*, 4493–4496; c) A. Lesage, L. Emsley, M. Chabanas, C. Copéret, J.-M. Basset, *Angew. Chem. Int. Ed.* **2002**, *41*, 4535–4538; d) M. Chabanas, A. Baudouin, C. Copéret, J.-M. Basset, W. Lukens, A. Lesage, S. Hediger, L. Emsley, *J. Am. Chem. Soc.* **2003**, *125*, 492–504.
- [89] S. Aime, A. Arce, R. Gobetto, D. Giusti, M. Stchedroff, *Chem. Commun.* **2000**, 1425–1426.
- [90] F. Rataboul, A. Baudouin, C. Thieuleux, L. Veyre, C. Copéret, J. Thivolle-Cazat, J.-M. Basset, A. Lesage, L. Emsley, *J. Am. Chem. Soc.* **2004**, *126*, 12541–12550.
- [91] D. Braga, L. Maini, M. Mazzotti, K. Rubini, A. Masic, R. Gobetto, F. Grepioni, *Chem. Commun.* **2002**, 2296–2297.
- [92] G. Kaupp, *CrystEngComm* **2003**, *5*, 117–133.
- [93] G. Rothenberg, A. P. Downie, C. L. Raston, J. L. Scott, *J. Am. Chem. Soc.* **2001**, *123*, 8701–8708.
- [94] D. Braga, S. L. Gialfreda, K. Rubini, F. Grepioni, M. R. Chierotti, R. Gobetto, *CrystEngComm* **2007**, *9*, 39–45.
- [95] V. P. Balema, J. W. Wiench, M. Pruski, V. K. Pecharsky, *Chem. Commun.* **2002**, 724–725.
- [96] V. P. Balema, J. W. Wiench, M. Pruski, V. K. Pecharsky, *Chem. Commun.* **2002**, 1606–1607.
- [97] V. P. Balema, J. W. Wiench, M. Pruski, V. K. Pecharsky, *J. Am. Chem. Soc.* **2002**, *124*, 6244–6245.
- [98] D. Braga, L. Maini, S. L. Gialfreda, F. Grepioni, M. R. Chierotti, R. Gobetto, *Chem. Eur. J.* **2004**, *10*, 3261–3269.
- [99] D. Braga, S. L. Gialfreda, F. Grepioni, M. R. Chierotti, R. Gobetto, G. Palladino, M. Polito, *CrystEngComm* **2007**, *9*, 879–881.
- [100] S. Yoshioka, Y. Aso, *J. Pharm. Sci.* **2007**, *96*, 960–981.
- [101] L. N. Bell, M. J. Hageman, *J. Agric. Food Chem.* **1994**, *42*, 2398–2401.
- [102] D. Braga, M. R. Chierotti, N. Garino, R. Gobetto, F. Grepioni, M. Polito, A. Viale, *Organometallics* **2007**, *26*, 2266–2271.
- [103] a) Y. Oprunenko, I. Gloriov, K. Lyssenko, S. Malyugina, D. Mityuk, V. Mstislavsky, H. Gunther, G. von Firks, M. Eberner, *J. Organomet. Chem.* **2002**, *656*, 27–42; b) Y. Oprunenko, *Russ. Chem. Bull.* **2002**, *51*, 907–929.
- [104] S. Aime, W. Dastrù, R. Gobetto, J. Krause, E. Sappa, *Organometallics* **1995**, *14*, 3224–3228.
- [105] a) See, for example: A. N. Sokolov, D. C. Swenson, L. R. MacGillivray, *Proc. Natl. Acad. Sci. USA* **2008**, *105*, 1794–1797, and references cited therein; b) J. A. R. P. Sarma, B. Chaudhuri, G. R. Desiraju, *Ind. J. Chem., A* **2000**, *39*, 253–261.
- [106] a) S. D. Karlen, M. A. Garcia-Garibay, *Top. Curr. Chem.* **2006**, *262*, 179–227; b) T. A. V. Khuong, J. E. Nunez, C. E. Godinez, M. A. Garcia-Garibay, *Acc. Chem. Res.* **2006**, *39*, 413–422.

Received: January 23, 2009  
Published Online: April 22, 2009